Theoretical Energy-Band Parameters for the Lead Salts

D. L. MITCHELL AND R. F. WALLIS
U. S. Naval Research Laboratory, Washington, D. C.
(Received 11 April 1966)

General expressions for the parabolic effective masses and g factors are obtained in terms of seven undetermined parameters for a six-band model at the L point of the NaCl lattice. The spin-orbit mixing of bands is treated explicitly with the result that both longitudinal and transverse components of the momentum are coupled between bands with L_6 symmetry and opposite parity. The six bands of interest are treated in the free-electron and tight-binding limits. The simplified expressions in the tight-binding limit, which approximate PbS, give spherical and nondegenerate valence- and conduction-band parameters. In this limit, the bands at L are similar in detail to certain of the bands at Γ in germanium and the III-V compounds. Expressions, valid over an extended range of $\mathbf{k}$, are also obtained for the nonparabolic effective masses and g factors. The signs of the g factors are treated in detail in order to resolve the differences which have appeared in the literature.

I. INTRODUCTION

THE lead salts are one of the oldest and most studied families of semiconductors[1] with applications which include the early crystal detectors,[2] infrared detectors,[3] and infrared lasers.[4] Only recently, however, have the main features of their band structure been determined.[5] This structure offers interesting contrasts to the corresponding band structures of the better known III-V compounds. The NaCl lattice of the lead salts has inversion symmetry in addition to the symmetry elements of the zinc-blende lattice of the III-V compounds, so that band extrema occur strictly at the Γ, L, and X symmetry points of the Brillouin zone and the twofold Kramers degeneracy is preserved at all points in the Brillouin zone. In contrast to the III-V compounds, which all have fourfold-degenerate valence bands at Γ with maxima nearby, the lead salts have twofold Kramers-degenerate valence-band maxima at the L point. The twofold-degenerate conduction-band minima are likewise at the L point with other energy bands energetically well separated. The absence of higher degeneracy leads to considerable simplification in treating physical processes involving the valence- and conduction-band extrema, particularly so in the case of PbS, where the bands are nearly spherical and nearly parabolic.

The one-electron band structure for the lead salts have been calculated theoretically using the cellular method (PbS),[6] the augmented-plane-wave (APW) method (PbTe),[7] and the pseudopotential method (PbS, PbSe, and PbTe).[8] The first calculation[6] is not in agreement with experiment. The discrepancy is probably due to the neglect of the relativistic mass-velocity and Darwin terms which are important for solids containing the heavier elements, such as lead.[9] The other band calculations are useful for establishing the gross order and spacing of the energy levels at selected points of the Brillouin zone but for a detailed description in the vicinity of band extrema it is more convenient to use $\mathbf{k}\cdot\mathbf{p}$ expressions for the effective mass and g-factor parameters. These parameters are measured directly by a variety of experiments.

There have been relatively few serious attempts to develop $\mathbf{k}\cdot\mathbf{p}$ expressions for the band parameters of the lead salts.[8,10,11] This is somewhat surprising considering the usefulness of these parameters to experimentalists. The problem, however, is not trivial since both the spin-orbit coupling and the magnetic field must be included properly in order to develop adequate expressions. The spin-orbit mixing of levels is of major importance since, in its absence, only the longitudinal (or the transverse) component of the momentum is coupled between a given pair of levels at the L point. Thus in general highly anisotropic bands would be expected. The magneto-optical experiments on PbS[12] and PbSe[13] give direct evidence that both components are coupled between the valence and conduction bands for these materials. Cuff *et al.*[14] suggested that the

[1] For a review of the work prior to 1959 see W. W. Scanlon, in *Solid State Physics*, edited by F. Seitz and D. Turnbull (Academic Press Inc., New York, 1959), Vol. 9, p. 83.
[2] L. W. Austin, Proc. IRE **7**, 257 (1919).
[3] T. S. Moss, Proc. Phys. Soc. (London) **62B**, 741 (1949).
[4] J. F. Butler, A. R. Calawa, R. J. Phelan, Jr., T. C. Harman, A. J. Strauss, and R. H. Rediker, Appl. Phys. Letters **5**, 75 (1964).
[5] For a summary of the most recent experimental and theoretical work see the several articles in *Proceedings of the International Conference of Semiconductor Physics, Paris, 1964* (Academic Press Inc., New York, 1964).
[6] D. G. Bell, D. M. Hum, L. Pincherle, D. W. Sciama, and P. M. Woodward, Proc. Roy. Soc. (London) **A217**, 71 (1953).
[7] J. B. Conklin, Jr., L. E. Johnson, and G. W. Pratt, Jr., Phys. Rev. **137**, A1282 (1965).
[8] P. J. Lin and L. Kleinman, Phys. Rev. **142**, 478 (1966).
[9] L. E. Johnson, J. B. Conklin, Jr., and G. W. Pratt, Jr., Phys. Rev. Letters **11**, 538 (1963); F. Herman, C. D. Kuglin, K. F. Cuff, and R. L. Kortum, *ibid.* **11**, 541 (1963).
[10] G. E. Pikus and G. L. Bir, Fiz. Tverd. Tela **3**, 2090 (1962) [English transl.: Soviet Phys.—Solid State **4**, 1530 (1963)] and G. L. Bir and G. E. Pikus, Fiz. Tverd. Tela **4**, 2243 (1962) [English transl.: Soviet Phys.—Solid State **4**, 1640 (1963)].
[11] J. O. Dimmock and G. B. Wright, Phys. Rev. **135**, A821 (1964).
[12] E. D. Palik, D. L. Mitchell, and J. N. Zemel, Phys. Rev. **135**, A763 (1964).
[13] D. L. Mitchell, E. D. Palik, and J. N. Zemel, in *Proceedings of the International Conference on the Physics of Semiconductors, Paris, 1964* (Academic Press Inc., New York, 1964), p. 325.
[14] K. F. Cuff, M. R. Ellett, C. D. Kuglin, and L. R. Williams, in *Proceedings of the International Conference on the Physics of Semiconductors, Paris, 1964* (Academic Press Inc., New York, 1964), p. 677.

spin-orbit mixing of bands is responsible for the regular decrease in band anisotropy for the lead-salt sequence PbTe; PbSe; PbS.

The $\mathbf{k}\cdot\mathbf{p}$ expressions for band parameters developed by Pikus and Bir[10] neglect the spin-orbit mixing of levels and do not include the full set of interacting bands. Dimmock and Wright[11] obtained the general parametrized $\mathbf{k}\cdot\mathbf{p}$ matrix including spin-orbit effects for the set of six interacting bands which they obtained in the free-electron limit. (The same bunched set of levels at the L point were also obtained by the other band calculations.[7,8]) In approximating this matrix for special cases, however, they likewise neglected the spin-orbit mixing of the symmetry states. In addition, their basis functions have incorrect spin assignments so that the derived g factors have incorrect signs. The same criticisms apply to the fragmentary calculation of Pratt and Ferreira.[15] The $\mathbf{k}\cdot\mathbf{p}$ portion of the most recent work[8] includes the spin-orbit mixing of levels but does not include expressions for all relevant bands, has major terms missing for the transverse g factor, and has $L_{4,5}$ basis functions which do not transform as labeled. In addition, the method of treating the spin-orbit mixing of bands is not clearly indicated.

None of the existing theory is adequate to treat the extensive magneto-optical experiments which have been done on the lead salts.[12,13] The present work obtains general expressions for the transverse and longitudinal effective mass and g-factor parameters for the six bands in terms of five adjustable momentum matrix elements and two spin-orbit mixing parameters. This reduces the number of undetermined parameters from the thirteen used by Dimmock and Wright[11] to seven with nonrestrictive approximations. Following Kane,[16] expressions for the nonparabolic effective mass and g-factor parameters are obtained which are valid over an extended region of the Brillouin zone. The double-group basis functions and the sign convention for the g factor are discussed in some detail since they have been the source of error in previous published work.

We also give a detailed discussion of the tight binding limit for bands originating from anion and cation p orbitals in the fcc lattice.[17] This model gives direct physical insight into band properties of the lead salts such as the occurance of nearly spherical bands with extrema at the L point. These insights are usually obscured by the computer band calculations. Our model, in the limit of large spin-orbit interaction, gives spherical-band extrema at the L point and thus clarifies the long-standing puzzle of the origin of nearly spherical bands in PbS.

[15] G. W. Pratt, Jr., and L. G. Ferreira, in *Proceedings of the International Conference on the Physics of Semiconductors, Paris, 1964* (Academic Press Inc., New York, 1964), p. 69.

[16] E. O. Kane, in *Physics of III-V Compounds*, edited by R. K. Willardson and A. C. Beer (Academic Press Inc., New York, to be published).

[17] D. L. Mitchell and R. F. Wallis, Bull. Am. Phys. Soc. **10**, 533 (1965).

II. THE k·p PERTURBATION MATRIX

The expansion of the energy levels of a crystal in the vicinity of a symmetry point in terms of the $\mathbf{k}\cdot\mathbf{p}$ perturbation has become a standard technique for determining band parameters in solids and the details will not be repeated here. Kane[16] has given a general review of the $\mathbf{k}\cdot\mathbf{p}$ representation, without magnetic fields, discussing the modifications introduced by spin-orbit (s.o.) coupling, exchange and many-electron effects. The magnetic field has been included in several treatments[18–21] which are reviewed and summarized by Yafet.[22] These treatments are similar in many respects to the $\mathbf{k}\cdot\mathbf{p}$ treatment, but differ in detail, depending on the particular representation chosen. We shall follow the treatment of Yafet[22] using the Luttinger-Kohn representation for which the matrix elements are defined in terms of the L-point Bloch functions. These functions are eigenfunctions of the usual one-electron Hamiltonian

$$H=p^2/2m_0+V(r)+(\hbar^2/4m_0^2c^2)(\nabla V\times\mathbf{p})\cdot\boldsymbol{\sigma}. \quad (2.1)$$

Recently, the importance of the relativistic mass-energy and Darwin terms have been demonstrated for fundamental band calculations.[9] These terms have the same symmetry as the potential and thus are automatically included in a semi-empirical $\mathbf{k}\cdot\mathbf{p}$ calculation which presupposes the symmetries and energies of the interacting bands.

A. Symmetries of Interacting Bands at L

The number of undefined matrix elements can be reduced by selecting basis functions which are eigenfunctions of the Hamiltonian without s.o. interaction and then diagonalizing the s.o. interaction with this basis.

If spin-orbit coupling is neglected, then the Bloch functions at the L point for the NaCl lattice are single-group (neglecting spin) nondegenerate representations of the group D_{3d} which transform like $L_1^{\pm}$, $L_2^{\pm}$, or doubly degenerate representations which transform like $L_3^{\pm}$.[23] Since there is inversion symmetry there will be an even (+) and odd (−) representation for each class. Dimmock and Wright[11] derived the symmetries for the six states in the vicinity of the Fermi level in the free-electron approximation. These states arise from Bloch functions of the form $\exp(i\mathbf{k}_0\cdot\mathbf{r})$, where $\mathbf{k}_0=\pm(\pi/a_0)[\bar{1}\bar{1}3]$ and cyclic permutations. Three of

[18] J. M. Luttinger and W. Kohn, Phys. Rev. **97**, 864 (1955).

[19] L. M. Roth, Phys. Rev. **118**, 1534 (1960); J. Phys. Chem. Solids **23**, 433 (1962).

[20] M. H. Cohen and E. I. Blount, Phil. Mag. **5**, 115 (1960).

[21] R. Bowers and Y. Yafet, Phys. Rev. **115**, 1165 (1959); Y. Yafet, *ibid.* **115**, 1172 (1959).

[22] Y. Yafet, in *Solid State Physics*, edited by F. Seitz and D. Turnbull (Academic Press Inc., New York, 1963), Vol. 14, p. 1.

[23] G. F. Koster, J. O. Dimmock, R. G. Wheeler, and H. Statz, *Properties of the Thirty-Two Point Groups* (M.I.T. Press, Cambridge, Massachusetts, 1963), p. 58.

these states are odd and transform like $Z(L_2^-)$ or $X\pm iY(L_3^-)$. The other three are even and transform like $R(L_1^+)$ or $S_X\pm iS_Y(L_3^+)$.[23] The X, Y, and Z coordinate axes are taken in the $[\bar{1}\bar{1}2]$, $[1\bar{1}0]$, and [111] crystallographic directions, respectively. The function R is invariant under the group of symmetry operations at L. S_X and S_Y transform like X and Y except they do not reverse sign under inversion,[24] i.e., S_X transforms like $YZ'-ZY'$ and S_Y like $ZX'-XZ'$.

Pratt *et al.*[7,15] and also Lin and Kleinman[8] arrive at the same set of symmetry states in the vicinity of the Fermi level. For PbTe they find that the even states are valence bands while the odd states are conduction bands. Furthermore, the six energy levels are clustered in a 3-eV spread, while the nearest other levels with nonzero $\mathbf{k}\cdot\mathbf{p}$ matrix elements are about 8 eV removed so that, for a $\mathbf{k}\cdot\mathbf{p}$ calculation, it is a good approximation to treat interactions among the six levels exactly and treat interactions with other levels by perturbation theory.[16]

B. Spin-Orbit Coupling

If the spin-orbit interaction is included, then the single group is no longer adequate to describe the transformation properties of the Bloch functions in a crystal. The double-group functions which do transform properly, however, may be derived from the single-group functions by including the spin indices $\uparrow$ and $\downarrow$. The double-group basis functions derived from the single-group functions listed above are given in Table I. The spin indices are

$$\uparrow=\begin{pmatrix}1\\0\end{pmatrix} \quad \text{and} \quad \downarrow=\begin{pmatrix}0\\1\end{pmatrix}$$

for σ_Z in the [111] crystallographic direction. The symbols $S_\pm$ and $X_\pm$ represent $(S_X\pm iS_Y)/\sqrt{2}$ and $(X\pm iY)/\sqrt{2}$, respectively.

The double-group basis functions we have selected differ in spin assignment from the double-group basis functions listed by Dimmock and Wright[11,25] and Pratt and Ferreira[15] who specifically have chosen a right-handed coordinate system. The $L_{4,5}$ functions differ from those listed by Lin and Kleinman.[8] We have verified our choice by generating the proper character under the point-group rotations at the L point. As an additional test we note that the two functions $Z\uparrow$ and $(X+iY)\downarrow$ are coupled by the s.o. interaction while $Z\uparrow$ and $(X-iY)\downarrow$ are not. Since the s.o. interaction only couples levels with the same symmetry, the first pair of functions are acceptable representations for L_6^- while the second pair are not. Reversing the spin assignment of the basis functions has the result (among others) of reversing the signs of the derived g factors so that the signs given by Pratt and Ferreira[15] are the reverse of those derived here.

With spin-orbit, the states at L have either $L_6^\pm$ or $L_{4,5}^\pm$ symmetry.[26] The L_6 states are twofold spin-degenerate states and representations can be found which are either "spin-up" or "spin-down." The L_4, L_5 states are each singly degenerate states and have both "spin-up" and "spin-down" components. However, these two states are Kramers-degenerate so that all states at the L point have the twofold Kramers degeneracy. This degeneracy is preserved at all points in the Brillouin zone for crystals with the NaCl lattice.

In addition to lifting the degeneracy of the $L_3^\pm$ levels, the spin-orbit coupling also mixes the states with $L_6^\pm$ symmetry which originate from different single-group states. It is this mixing which allows coupling of both longitudinal and transverse components of the momentum matrix elements so that spherical, or nearly spherical bands may result from the $\mathbf{k}\cdot\boldsymbol{\pi}$ interaction of a single pair of levels at the L point.[27] It is also likely that such a mixing is also responsible for the observed feature in bismuth that the transverse g factor is nearly twice the reciprocal of the corresponding cyclotron mass ratio, a relation only expected to be true for $\mathbf{k}\cdot\boldsymbol{\pi}$ interaction between a single pair of bands.[22]

The matrix elements of the Hamiltonian at the L point, including s.o. coupling, are given in Table I for the even and odd set of states. The nonzero s.o. matrix elements are obtained by noting that the s.o. operator can be written $\boldsymbol{\Sigma}\cdot\boldsymbol{\sigma}$, where Σ_Z transforms like S_Z and $\Sigma_X\pm i\Sigma_Y$ transform like $S_X\pm iS_Y$. The s.o. Hamiltonians given in Table I neglect interactions with bands not included in the initial set. In the lead salts the next-nearest states at the L point are about 5 eV removed[7,8] while the s.o. energies are of the order of 1 eV or less.

Within this approximation, the s.o. Hamiltonians for the valence and conduction bands are diagonalized by the symmetry functions and energies:

$$\begin{aligned}
&L_{61}^+\beta = i(\cos\theta^+)R\downarrow + (\sin\theta^+)S_-\uparrow,\\
&L_{61}^-\beta = (\cos\theta^-)Z\downarrow + (\sin\theta^-)X_-\uparrow,\\
&\quad \epsilon_1^\pm = \epsilon_0^\pm\cos^2\theta^\pm - \Delta_1^\pm\sin^2\theta^\pm + 2\sqrt{2}\Delta_2^\pm\sin\theta^\pm\cos\theta^\pm,\\
&L_{62}^+\beta = i(\sin\theta^+)R\downarrow - (\cos\theta^+)S_-\uparrow,\\
&L_{62}^-\beta = (\sin\theta^-)Z\downarrow - (\cos\theta^-)X_-\uparrow,\\
&\quad \epsilon_2^\pm = \epsilon_0^\pm\sin^2\theta^\pm - \Delta_1^\pm\cos^2\theta^\pm - 2\sqrt{2}\Delta_2^\pm\sin\theta^\pm\cos\theta^\pm,\\
&L_4^+\beta = (2)^{-1/2}[S_+\uparrow - iS_-\downarrow],\\
&L_4^-\beta = (2)^{-1/2}[X_+\uparrow - iX_-\downarrow],\\
&\quad \epsilon_3^\pm = \Delta_1^\pm,
\end{aligned} \tag{2.2}$$

[24] Reference 23, p. 58.

[25] J. O. Dimmock (private communication) has verified our assignment by an independent calculation. The general $\mathbf{k}\cdot\mathbf{p}$ matrix in their paper is valid provided the $\kappa_\pm$ labels are interchanged.

[26] The labeling of the double-group states for D_{3d} conforms with the published articles but differs with Koster *et al.* (Ref. 23). The $L_4^\pm$, $L_5^\pm$, and $L_6^\pm$ states correspond to Koster's $\Gamma_5^\pm$, $\Gamma_6^\pm$, and $\Gamma_4^\pm$ states, respectively.

[27] In $\mathbf{k}\cdot\mathbf{p}$ treatments which ignore such mixing one of these contributions to the effective mass and g factor is assigned to interactions with "distant" bands. If not applied properly, such treatments can lead to incorrect estimates of the momentum matrix element between a given band and the "distant" band.

TABLE I. The matrix elements of the Hamiltonian including s.o. are given for the L point in terms of the basis functions: $L_6^+(L_1^+)\uparrow,\downarrow = -iR\uparrow, iR\downarrow$; $L_6^+(L_3)\uparrow,\downarrow = S_-\uparrow, S_+\downarrow$; $L_4^+ = (2)^{-1/2}[S_+\uparrow - iS_-\downarrow]$; $L_5^+ = (2)^{-1/2}[iS_+\uparrow - S_-\downarrow]$; $L_6^-(L_2^-)\uparrow,\downarrow = Z\uparrow,\downarrow$; $L_6^-(L_3^-)\uparrow,\downarrow = X_-\uparrow, X_+\downarrow$; $L_4^- = (2)^{-1/2}[X_+\uparrow - iX_-\downarrow]$, $L_5^- = (2)^{-1/2}[iX_+\uparrow - X_-\downarrow]$. The zero-in-energy for the even or for the odd set of levels is taken at the position of the L_3^+ or L_3^- levels neglecting s.o. coupling. The energy ϵ_0^+ or ϵ_0^- is the position of the L_1^+ or L_2^- level with respect to the corresponding zero. The nonzero matrix elements of the s.o. operator are: $\langle S_Y|\Sigma_Z|S_X\rangle = -\langle S_X|\Sigma_Z|S_Y\rangle = i\Delta_1^+$; $\langle Y|\Sigma_Z|X\rangle = -\langle X|\Sigma_Z|Y\rangle = i\Delta_1^-$; $\langle R|\Sigma_X|S_X\rangle = \langle R|\Sigma_Y|S_Y\rangle = i\Delta_2^+$; $\langle Z|\Sigma_X|Y\rangle = -\langle Z|\Sigma_Y|X\rangle = i\Delta_2^+$.

	$L_6^\pm(L_{1,2}^\pm)\uparrow$	$L_6^\pm(L_{1,2}^\pm)\downarrow$	$L_6^\pm(L_3^\pm)\uparrow$	$L_6^\pm(L_3^\pm)\downarrow$	$L_4^\pm$	$L_5^\pm$
$L_6^\pm(L_{1,2}^\pm)\uparrow$	$\epsilon_0^\pm$	0	0	$-\sqrt{2}\Delta^\pm$	0	0
$L_6^\pm(L_{1,2}^\pm)\downarrow$	0	$\epsilon_0^\pm$	$\sqrt{2}\Delta_2^\pm$	0	0	0
$L_6^\pm(L_3^\pm)\uparrow$	0	$\sqrt{2}\Delta_2^\pm$	$-\Delta_1^\pm$	0	0	0
$L_6^\pm(L_3^\pm)\downarrow$	$-\sqrt{2}\Delta_2^\pm$	0	0	$-\Delta_1^\pm$	0	0
$L_4^\pm$	0	0	0	0	$\Delta_1^\pm$	0
$L_5^\pm$	0	0	0	0	0	$\Delta_1^\pm$

where the basis functions and nonzero matrix elements are given in the caption to Table I. The zero-in-energy for each set of levels is chosen at the location of the corresponding L_3^+ and L_3^- level before application of the spin-orbit interaction. Similarly $\epsilon_0^\pm$ represent the energies of the corresponding L_1^+ and L_2^- levels relative to these zeros. The $L_4^\pm$, $L_5^\pm$ levels are unmixed by s.o. and retain the eigenvalues $\Delta_1^\pm$.

Only the $L_i^\pm\beta$ functions are listed in Eq. (2.2) for each Kramers conjugate pair. The other function of each pair ($L_i^\pm\alpha$) is obtained by applying the time-reversal operator $K = i\sigma_y K_0$ to the given function,[22] where K_0 is the operator for taking the complex conjugate. For a general point in the Brillouin zone, this operation generates a state at $-\mathbf{k}$. However, $\mathbf{k}$ and $-\mathbf{k}$ are equivalent at the L point so that Kramers conjugation generates states of the same $\mathbf{k}$ vector just as at the Γ point ($k=0$). The α, β labels have been chosen for the mixed "spin-up," "spin-down" functions so that they have the same symmetry under time reversal as the pure spin states $\uparrow$, $\downarrow$, i.e., $K\beta=\alpha$, $K\alpha=-\beta$.

It is worth noting that the spin-orbit coupling mixes "spin-up" components of the $L_6^\pm$ states which arise from L_1^+ or L_2^- with the "spin-down" of the $L_6^\pm$ states which arise from L_3^+ or L_3^-. The four pairs of functions which result $L_{61}^\pm$ and $L_{62}^\pm$ may still be labeled as Kramers conjugate pairs with labels α, β, although the $\uparrow$, $\downarrow$ labels are no longer adequate. The relative mixing of the states by the s.o. coupling is expressed in terms of the parameter $\theta^\pm$, where

$$\tan 2\theta^\pm = 2\sqrt{2}\Delta_2^\pm(\epsilon_0^\pm + \Delta_1^\pm)^{-1}. \tag{2.3}$$

It is instructive to consider the weak and strong s.o. coupling limits for the odd states which are assumed to originate from three degenerate p-like states in the tight binding limit. The twofold spin degeneracy is neglected in this discussion since it is present for all states at Γ and L. In germanium and III-V compounds these are the triply degenerate valence bands at Γ, if s.o. coupling is ignored. The s.o. coupling splits the valence bands into an upper, doubly degenerate level and a lower, nondegenerate level. The s.o. Hamiltonian given in Table I is equivalent to the s.o. Hamiltonian for the valence band in InSb[28] in the limit $\Delta_2^- \to \Delta_1^-$ and $\epsilon_0^- \to 0$. At the L point, the p-like bands without s.o. coupling are split into a doubly degenerate level and a nondegenerate level (neglecting spin) with an energy separation ϵ_0^-. The mixing parameter θ^- is zero in this case. If the s.o. coupling is large and positive then the upper two levels are separated by $\frac{2}{3}\epsilon_0^-$ and are removed from the lower level by $3\Delta_1^-$ (note that the s.o. parameter Δ_1^- used in this paper is $\frac{1}{3}$ the value often employed). The mixing parameter for this case is given by $\sin\theta^- = 1/\sqrt{3}$. This second case appears to apply to the conduction band in PbS and, with an appropriate order of levels in the valence band, gives spherical or nearly spherical bandedge parameters. Thus, in the limit of the crystal-field splitting small compared to the s.o. splitting, the basis functions for the split-off band at L are the same as for the split-off band at Γ in InSb.[28]

TABLE II. Transformation of the coordinate functions under the rotations Q_i and of the spin states $\uparrow$ and $\downarrow$ under the corresponding spinor transformations S_i^{-1}. The operators Q_2, Q_3, and $Q_4(3C_2)$ generate proper rotations of 180° about the stated crystal axis. The operators Q_5 and $Q_6(2C_3)$ generate rotations of 120° about the $[\bar{1}11]$ axis. The phase parameter $\omega = \exp(i2\pi/3)$.

	S_2^{-1} $Q_2[1\bar{1}0]$	S_3^{-1} $Q_3[\bar{1}01]$	S_4^{-1} $Q_4[0\bar{1}1]$	S_5^{-1} $Q_5[111]^+$	S_6^{-1} $Q_6[111]^-$
Z	$-Z$	$-Z$	$-Z$	Z	Z
X_+	$-X_-$	$-\omega X_-$	$-\omega^* X_-$	ωX_+	$\omega^* X_+$
R	R	R	R	R	R
S_-	$-S_+$	$-\omega^* S_+$	$-\omega S_+$	$\omega^* S_-$	ωS_-
α	$\mp\beta$	$\mp\omega^*\beta$	$\mp\omega\beta$	$\mp\omega^*\alpha$	$\mp\omega\alpha$
β	$\pm\alpha$	$\pm\omega\alpha$	$\pm\omega^*\alpha$	$\mp\omega\beta$	$\mp\omega^*\beta$

[28] E. O. Kane, J. Phys. Chem. Solids 1, 249 (1957).

TABLE III. The matrix elements $\langle L_i^+|\kappa\cdot\pi|L_j^-\rangle$ are listed for the s.o. mixed functions defined by Eqs. (2.2). The s.o. mixing parameters $\theta^\pm$ are defined in Eq. (2.3) and the momentum matrix elements P_{ij} are defined in Eq. (2.4). The $K_\pm$ represent $(K_X \pm iK_Y)/\sqrt{2}$.

	$L_{61}^-\alpha$	$L_{61}^-\beta$	$L_{62}^-\beta$
$L_{61}^+\alpha$	$+[(\cos\theta^+\cos\theta^-)P_{11}+(\sin\theta^+\sin\theta^-)P_{21}]K_Z$	$+[(\cos\theta^+\sin\theta^-)P_{13}-(\sin\theta^+\cos\theta^-)P_{31}]K_-$	$-[(\cos\theta^+\cos\theta^-)P_{13}+(\sin\theta^+\sin\theta^-)P_{31}]K_-$
$L_{61}^+\beta$	$+[(\cos\theta^+\sin\theta^-)P_{13}-(\sin\theta^+\cos\theta^-)P_{31}]K_+$	$+[(\cos\theta^+\cos\theta^-)P_{11}+(\sin\theta^+\sin\theta^-)P_{21}]K_Z$	$-[(\cos\theta^+\sin\theta^-)P_{11}-(\sin\theta^+\cos\theta^-)P_{21}]K_Z$
$L_{62}^+\beta$	$+[(\cos\theta^+\cos\theta^-)P_{31}+(\sin\theta^+\sin\theta^-)P_{13}]K_+$	$+[(\cos\theta^+\sin\theta^-)P_{21}-(\sin\theta^+\cos\theta^-)P_{11}]K_Z$	$-[(\cos\theta^+\cos\theta^-)P_{21}+(\sin\theta^+\sin\theta^-)P_{11}]K_Z$
$L_{62}^+\alpha$	$-[(\cos\theta^+\sin\theta^-)P_{21}-(\sin\theta^+\cos\theta^-)P_{11}]K_Z$	$+[(\cos\theta^+\cos\theta^-)P_{31}+(\sin\theta^+\sin\theta^-)P_{13}]K_-$	$+[(\cos\theta^+\sin\theta^-)P_{31}-(\sin\theta^+\cos\theta^-)P_{13}]K_-$
$L_4^+\beta$	$+[(\cos\theta^-)P_{31}/\sqrt{2}-i(\sin\theta^-)P_{22}]K_-$	$-i[(\cos\theta^-)P_{31}/\sqrt{2}-i(\sin\theta^-)P_{22}]K_+$	$-i[(\sin\theta^-)P_{31}/\sqrt{2}+i(\cos\theta^-)P_{22}]K_+$
$L_5^+\alpha$	$-i[(\cos\theta^-)P_{31}/\sqrt{2}+i(\sin\theta^-)P_{22}]K_-$	$+[(\cos\theta^-P_{31}/\sqrt{2}+i(\sin\theta^-)P_{22}]K_+$	$+[(\sin\theta^-)P_{31}/\sqrt{2}-i(\cos\theta^-)P_{22}]K_+$
	$L_{62}^-\alpha$	$L_4^-\beta$	$L_5^-\alpha$
$L_{61}^+\alpha$	$+[(\cos\theta^+\sin\theta^-)P_{11}-(\sin\theta^+\cos\theta^-)P_{21}]K_Z$	$+[(\cos\theta^+)P_{13}/\sqrt{2}-i(\sin\theta^+)P_{22}]K_+$	$+[i(\cos\theta^+)P_{13}/\sqrt{2}-(\sin\theta^+)P_{22}]K_+$
$L_{61}^+\beta$	$-[(\cos\theta^+\cos\theta^-)P_{13}+(\sin\theta^+\sin\theta^-)P_{31}]K_+$	$+[i(\cos\theta^+)P_{13}/\sqrt{2}+(\sin\theta^+)P_{22}]K_-$	$+[(\cos\theta^+)P_{13}/\sqrt{2}+i(\sin\theta^+)P_{22}]K_-$
$L_{62}^+\beta$	$+[(\cos\theta^+\sin\theta^-)P_{31}-(\sin\theta^+\cos\theta^-)P_{13}]K_+$	$+i[(\sin\theta^+)P_{13}/\sqrt{2}+i(\cos\theta^+)P_{22}]K_-$	$+[(\sin\theta^+)P_{13}/\sqrt{2}-i(\cos\theta^+)P_{22}]K_-$
$L_{62}^+\alpha$	$+[(\cos\theta^+\cos\theta^-)P_{21}+(\sin\theta^+\sin\theta^-)P_{11}]K_Z$	$+[(\sin\theta^+)P_{13}/\sqrt{2}+i(\cos\theta^+)P_{22}]K_+$	$+i[(\sin\theta^+)P_{13}/\sqrt{2}-i(\cos\theta^+)P_{22}]K_+$
$L_4^+\beta$	$+[(\sin\theta^-)P_{31}/\sqrt{2}+i(\cos\theta^-)P_{22}]K_-$	0	$+iP_{21}K_Z$
$L_5^+\alpha$	$-i[(\sin\theta^-)P_{31}/\sqrt{2}-i(\cos\theta^-)P_{22}]K_-$	$-iP_{21}K_Z$	0

The case described here corresponds to the tight-binding limit for odd bands at L which originate from the lead p orbitals (see Sec. III B). Lin and Kleinman[8] arrive at a different composition for the lowest conduction band in PbS. Their composition for the conduction band corresponds to a mixing parameter $\sin\theta^-\approx\sqrt{\frac{2}{3}}$ which would require an appreciable crystal field splitting ϵ_0^-.

C. Symmetry-Allowed π Matrix Elements

The energies of the bands in the vicinity of the L point can be expressed in terms of the matrix elements of the perturbation $\kappa\cdot\pi$ evaluated at L. The operator π is the operator $\mathbf{p}+\sigma\times\nabla V(\hbar/4m_0c^2)$ and κ is the wave vector relative to L.[22] The $\kappa\cdot\pi$ matrix elements for the s.o. mixed double-group states can be reduced to sums of the symmetry allowed π matrix elements for the single-group states $L_1^\pm$, $L_2^\pm$, and $L_3^\pm$. The procedure has the advantage of reducing the number of undetermined π matrix elements to a minimum and also of expressing them in a form suitable for further reduction in limiting approximations.

The nonzero matrix elements of π may be obtained directly from the tables of coupling coefficients for the single-group states of D_{3d}[23] by noting that π_Z transforms like L_2^- and $\pi_\pm=(\pi_X\pm i\pi_Y)/\sqrt{2}$ transform like $L_{3\pm}^-$. The nonzero matrix elements are $\langle L_1^+|L_2^-|L_2^-\rangle$, $\langle L_1^+|L_{3\pm}^-|L_{3\mp}^-\rangle$, $\langle L_{3\pm}^{+*}|L_2^-|L_{3\pm}^-\rangle$, $\langle L_{3\pm}^{+*}|L_{3\pm}^-|L_2^-\rangle$, and $\langle L_{3\pm}^{+*}|L_{3\mp}^-|L_{3\mp}^-\rangle$. Since π is an odd operator, only states with opposite parity are coupled.

Alternatively, the nonzero matrix elements can be obtained from the transformation properties of the basis functions R, $S_\pm$, Z, and $S_\pm$ under the symmetry operations of the group D_{3d}. These are listed in Table II for the pertinent coordinate transformations Q_2, Q_3, and $Q_4(3C_2)$, which are rotations of 180° about the $[1\bar{1}0]$, $[\bar{1}01]$, and $[0\bar{1}1]$ axes, respectively, and for Q_5 and $Q_6(2C_3)$, which are rotations of 120° about the [111] axis. The transformation properties of the spin states $\uparrow$ and $\downarrow$ under the corresponding operations S_1^{-1}, which generate the double group, are also given.

The nonzero π matrix elements for the functions listed in Table II are

$$\begin{aligned}
\langle R|\pi_Z|Z\rangle &= -iP_{11},\\
\langle R|\pi_\pm|X_\mp\rangle &= -iP_{13},\\
\langle S_\pm^*|\pi_Z|X_\pm\rangle &= \pm P_{21},\\
\langle S_\pm^*|\pi_\pm|Z\rangle &= \pm P_{31},\\
\langle S_\pm^*|\pi_\mp|X_\mp\rangle &= \mp\sqrt{2}P_{22},
\end{aligned} \tag{2.4}$$

where the constants P_{ij} are real if π is a purely imaginary operator.

D. The $\kappa\cdot\pi$ Perturbation Matrix

The $\kappa\cdot\pi$ matrix elements between the s.o. mixed states listed in Eq. (2.2) are given in Table III in terms of the five symmetry-allowed π matrix elements given by Eq. (2.4). Table III has been constructed so that all parameters are real. It is to be noted that Table III is not the full $\kappa\cdot\pi$ perturbation matrix, which is 12×12, although the full matrix may be constructed from the elements given here. The set of matrix elements is a specific representation of the general set presented by Dimmock and Wright.[11,25] Instead of thirteen general parameters, we have particularized the set in terms of five momentum matrix elements and two s.o. mixing coefficients. This reduction is due to the neglect of s.o. interactions with other bands not included in the initial set.

E. Effective Masses and g Factors

The energy levels for a crystal in the vicinity of the L point are obtained by diagonalizing the $\kappa\cdot\pi$ matrix derived from Table III. The procedure for doing this in the presence of a magnetic field is detailed by Yafet.[22] The effect of the magnetic field is included by adding to the wave vector κ the Lorentz term $(e/\hbar c)\mathbf{A}(i\nabla_\kappa)$, where the magnetic field part of the vector potential $\mathbf{A}$ is considered to be a function of the operator $i\nabla_\kappa$. With this substitution, the energy levels to lowest order in the $\kappa\cdot\pi$ perturbation for a specific band n are deter-

mined by the 2×2 operator equation[22]

$$E_{n\rho;n\rho'}(\mathbf{K})=E_n(\mathbf{k}_0)\delta_{\rho,\rho'}+\frac{\hbar^2}{2m_0}\sum_i\sum_{m,\rho'}\left\{1+2\frac{\langle n,\rho|\pi^i(\mathbf{k}_0)|m,\rho'\rangle\langle m,\rho'|\pi^i(\mathbf{k}_0)|n,\rho\rangle}{[E_n(\mathbf{k}_0)-E_m(\mathbf{k}_0)]m_0}\right\}\mathrm{K}_i^2$$
$$-\frac{i\hbar^2}{2m_0}\sum_{i<j}\sum_{m,\rho''}\frac{2\langle n,\rho|\pi^i(\mathbf{k}_0)|m,\rho''\rangle\langle m,\rho''|\pi^j(\mathbf{k}_0)|n,\rho'\rangle s\lambda_k\epsilon_{ijk}}{[E_n(\mathbf{k}_0)-E_m(\mathbf{k}_0)]m_0}+\frac{g_0\beta H}{2}\sum_i\lambda_i\langle n,\rho|\sigma^i|n,\rho'\rangle, \quad (2.5)$$

where $E_n(\mathbf{k}_0)$ are the energies of the bands at the L point, ρ and ρ' label the two Kramers-degenerate states for each band, i and j are Cartesian labels X, Y, Z, s is $eH/\hbar c$, $\mathbf{K}=\boldsymbol{\kappa}+(e/\hbar c)\mathbf{A}(i\nabla_\kappa)$, λ_i are the direction cosines of the magnetic field with respect to the Cartesian axes $\mathbf{i}$, σ^i are the Cartesian components of the spin operator, m_0 and g_0 are the free-electron mass and g factor, respectively, ϵ_{ijk} is the Levi-Civita or permutation index, and π^i are the Cartesian components of the momentum matrix element evaluated at the L point.

The effective masses and g factors, for a given band n, may be obtained directly from Eq. (2.5) in the parabolic approximation, i.e., $|E_n(\boldsymbol{\kappa})-E_n(\mathbf{k}_0)| \ll |E_n(\mathbf{k}_0)-E_m(\mathbf{k}_0)|$ for all bands m. Nonparabolic effects arising from the $\boldsymbol{\kappa}\cdot\boldsymbol{\pi}$ interaction between a single pair of levels may be treated in a simple manner and are considered in a later section. The transverse and longitudinal reciprocal mass ratios $(m_0/m_n^{t,l})$ for a given band n are given directly by the sum inside curly brackets which appears in the second term of Eq. (2.5). (The magnetic field is taken equal to zero.) The interband matrix elements which appear in the sum were obtained from Eq. (2.4). The results are tabulated in Table IV in terms of the undetermined matrix elements and mixing coefficients defined previously. No restriction has been placed on the relative ordering of the energy levels. Thus a negative sign for the energy difference E_n-E_m results in a negative contribution to the "electronic" effective mass (or a positive contribution to a "hole" mass).

With a nonzero magnetic field, the Kramers degeneracy is lifted by the last two terms appearing in Eq. (2.5). The magnitude of the g factor, for a given band, is specified by the difference in energy between the two levels. The sign of the g factor, however, is not uniquely defined and must be established by convention since the "spin-up" or "spin-down" directions are not uniquely specified for the s.o. mixed states.

1. Sign Conventions for g Factor

The sign of the g factor, for states which have only twofold Kramers-degeneracy in the absence of s.o. interaction, may be determined by requiring the g factor to approach the "free-electron" value of +2 in the limit of zero s.o. interaction. This convention is adequate for the $L_{61}^{\pm}$ levels but is not appropriate for the $L_{62}^{\pm}$ or $L_{4,5}^{\pm}$ levels which have higher than twofold degeneracy in the absence of s.o. interaction.

An alternative convention specifies the sign of the g factor in terms of the sense of the circularly polarized radiation absorbed in spin-resonance transitions.[22] The magnetic-dipole matrix element for "free-electron" spin resonance is proportional to $\langle\uparrow|\sigma_+|\downarrow\rangle$, where $\sigma_\pm=(\sigma_X\pm i\sigma_Y)/2$ for a magnetic field in the $+Z$ direction and where the $\uparrow$ state lies to higher energy. The plus or minus signs refer to left- or right-circularly polarized radiation, respectively. All other matrix elements of $\sigma_\pm$ for $\uparrow$, $\downarrow$ states are zero so that the "up" state and "down" state are uniquely specified. Similarly, the mixed-spin states with Kramers labels α or β can be given an unique "up" or "down" designation if only a single-matrix element of σ_+ is nonzero. The sign of the g factor is then positive if the $\uparrow$ state lies to higher energy. This second convention gives the same sign for the $L_{61}^{\pm}$ levels in the limit of weak s.o. interaction as the first convention. In the limit of strong s.o. interaction [i.e., $\Delta\gg\epsilon$ in Eq. (2.3)] this second convention also uniquely specifies the "up" and "down" states for the $L_{62}^{\pm}$ levels. In anticipation of the results of the next section, which give a "spherical approximation" for valence- and conduction-band edges at the L point, we have chosen the sign convention according to the weak s.o. limit for the even (+) states and strong s.o. limit for the odd (−) states. The formulas for the longitudinal and transverse g factors for the several bands are listed in Table IV. The sign of the g factor for the $L_{4,5}^{\pm}$ levels has been left undetermined since it is not uniquely defined in either of the two s.o. limits.

There are some questions in the literature concerning the signs of the g factors in the lead salts.[7,8,14] The signs have been determined experimentally for PbS[12] by observing the influence of band population on the interband Landau transitions. The same signs have been suggested for PbSe[13] since the sign of the interband Faraday rotation is the same. This assignment of signs, negative for valence band and positive for the conduction band, for the longitudinal g factor is the same as that given by the equations in Table IV which were derived using the sign convention described above.

In fact, the sign and magnitude of the contribution to the longitudinal g factor from the interaction between a valence band with $L_6^{\pm}$ symmetry and a conduction band with $L_6^{\mp}$ symmetry are both given by $g_{v,c}^{\,l}=2m_0/m_{v,c}^{\,t}$ where $m_v^{\,t}$ for electrons is negative. This

TABLE IV. The general expressions for the longitudinal and transverse effective masses are given under the heading "effective mass" for the six L-point states defined in the text. The states are identified by the energy labels defined in Eqs. (2.2). The expressions for the longitudinal and transverse g factors are given under the heading "g factor." The algebraic signs given refer to electronic states, i.e., the valence-band masses are negative. The sign convention for the g factors is described in the text.

Effective Mass

$$\frac{m_0}{m_{61+}{}^t}=1+\frac{1}{2m_0}\left\{\frac{2[(\cos\theta^+\sin\theta^-)P_{13}-(\sin\theta^+\cos\theta^-)P_{31}]^2}{\epsilon_1{}^+-\epsilon_1{}^-}+\frac{2[(\cos\theta^+\cos\theta^-)P_{13}+(\sin\theta^+\sin\theta^-)P_{31}]^2}{\epsilon_1{}^+-\epsilon_2{}^-}+\frac{4[(\cos^2\theta^+)P_{13}{}^2/2+(\sin^2\theta^+)P_{22}{}^2]}{\epsilon_1{}^+-\epsilon_3{}^-}\right\},$$

$$\frac{m_0}{m_{61+}{}^l}=1+\frac{1}{2m_0}\left\{\frac{4[(\cos\theta^+\cos\theta^-)P_{11}+(\sin\theta^+\sin\theta^-)P_{21}]^2}{\epsilon_1{}^+-\epsilon_1{}^-}+\frac{4[(\cos\theta^+\sin\theta^-)P_{11}-(\sin\theta^+\cos\theta^-)P_{21}]^2}{\epsilon_1{}^+-\epsilon_2{}^-}\right\},$$

$$\frac{m_0}{m_{62+}{}^t}=1+\frac{1}{2m_0}\left\{\frac{2[(\cos\theta^+\cos\theta^-)P_{31}+(\sin\theta^+\sin\theta^-)P_{13}]^2}{\epsilon_2{}^+-\epsilon_1{}^-}+\frac{2[(\cos\theta^+\sin\theta^-)P_{31}-(\sin\theta^+\cos\theta^-)P_{13}]^2}{\epsilon_2{}^+-\epsilon_2{}^-}+\frac{4[(\sin^2\theta^+)P_{13}{}^2/2+(\cos^2\theta^+)P_{22}{}^2]}{\epsilon_2{}^+-\epsilon_3{}^-}\right\},$$

$$\frac{m_0}{m_{62+}{}^l}=1+\frac{1}{2m_0}\left\{\frac{4[(\cos\theta^+\sin\theta^-)P_{21}-(\sin\theta^+\cos\theta^-)P_{11}]^2}{\epsilon_2{}^+-\epsilon_1{}^-}+\frac{4[(\cos\theta^+\cos\theta^-)P_{21}+(\sin\theta^+\sin\theta^-)P_{11}]^2}{\epsilon_2{}^+-\epsilon_2{}^-}\right\},$$

$$\frac{m_0}{m_{4,5+}{}^t}=1+\frac{1}{2m_0}\left\{\frac{4[(\cos^2\theta^-)P_{31}{}^2/2+(\sin^2\theta^-)P_{22}{}^2]}{\epsilon_3{}^+-\epsilon_1{}^-}+\frac{4[(\sin^2\theta^-)P_{31}{}^2/2+(\cos^2\theta^-)P_{22}{}^2]}{\epsilon_3{}^+-\epsilon_2{}^-}\right\},$$

$$\frac{m_0}{m_{4,5+}{}^l}=1+\frac{1}{2m_0}\left\{\frac{4P_{21}{}^2}{\epsilon_3{}^+-\epsilon_3{}^-}\right\},$$

$$\frac{m_0}{m_{61-}{}^t}=1+\frac{1}{2m_0}\left\{\frac{2[(\cos\theta^+\sin\theta^-)P_{13}-(\sin\theta^+\cos\theta^-)P_{31}]^2}{\epsilon_1{}^--\epsilon_1{}^+}+\frac{2[(\cos\theta^+\cos\theta^-)P_{31}+(\sin\theta^+\sin\theta^-)P_{13}]^2}{\epsilon_1{}^--\epsilon_2{}^+}+\frac{4[(\cos^2\theta^-)P_{31}{}^2/2+(\sin^2\theta^-)P_{22}{}^2]}{\epsilon_1{}^--\epsilon_3{}^+}\right\},$$

$$\frac{m_0}{m_{61-}{}^l}=1+\frac{1}{2m_0}\left\{\frac{4[(\cos\theta^+\cos\theta^-)P_{11}+(\sin\theta^+\sin\theta^-)P_{21}]^2}{\epsilon_1{}^--\epsilon_1{}^+}+\frac{4[(\cos\theta^+\sin\theta^-)P_{21}-(\sin\theta^+\cos\theta^-)P_{11}]^2}{\epsilon_1{}^--\epsilon_2{}^+}\right\},$$

$$\frac{m_0}{m_{62-}{}^t}=1+\frac{1}{2m_0}\left\{\frac{2[(\cos\theta^+\cos\theta^-)P_{13}+(\sin\theta^+\sin\theta^-)P_{31}]^2}{\epsilon_2{}^--\epsilon_1{}^+}+\frac{+2[(\cos\theta^+\sin\theta^-)P_{31}-(\sin\theta^+\cos\theta^-)P_{13}]^2}{\epsilon_2{}^--\epsilon_2{}^+}+\frac{4[(\sin^2\theta^-)P_{31}{}^2/2+(\cos^2\theta^-)P_{22}{}^2]}{\epsilon_2{}^--\epsilon_3{}^+}\right\},$$

$$\frac{m_0}{m_{62-}{}^l}=1+\frac{1}{2m_0}\left\{\frac{4[(\cos\theta^+\sin\theta^-)P_{11}-(\sin\theta^+\cos\theta^-)P_{21}]^2}{\epsilon_2{}^--\epsilon_1{}^+}+\frac{4[(\cos\theta^+\cos\theta^-)P_{21}+(\sin\theta^+\sin\theta^-)P_{11}]^2}{\epsilon_2{}^--\epsilon_2{}^+}\right\},$$

$$\frac{m_0}{m_{4,5-}{}^t}=1+\frac{1}{2m_0}\left\{\frac{4[(\cos^2\theta^+)P_{13}{}^2/2+(\sin^2\theta^-)P_{22}{}^2]}{\epsilon_3{}^--\epsilon_1{}^+}+\frac{4[(\sin^2\theta^+)P_{13}{}^2/2+(\cos^2\theta^+)P_{22}{}^2]}{\epsilon_3{}^--\epsilon_2{}^+}\right\},$$

$$\frac{m_0}{m_{4,5-}{}^l}=1+\frac{1}{2m_0}\left\{\frac{4P_{21}{}^2}{\epsilon_3{}^--\epsilon_3{}^+}\right\}.$$

⟨g Factor⟩

$$g_{61+}{}^l=2(\cos^2\theta^+-\sin^2\theta^+)+\frac{1}{2m_0}\left\{\frac{4[(\cos\theta^+\sin\theta^-)P_{13}-(\sin\theta^+\cos\theta^-)P_{31}]^2}{\epsilon_1{}^+-\epsilon_1{}^-}+\frac{4[(\cos\theta^+\cos\theta^-)P_{13}+(\sin\theta^+\sin\theta^-)P_{31}]^2}{\epsilon_1{}^+-\epsilon_2{}^-}-\frac{8[(\cos^2\theta^+)P_{13}{}^2/2+(\sin^2\theta^+)P_{22}{}^2]}{\epsilon_1{}^+-\epsilon_3{}^-}\right\},$$

$$g_{61+}{}^t=2\cos^2\theta^+-\frac{1}{2m_0}\left\{\frac{4\sqrt{2}[(\cos\theta^+\sin\theta^-)P_{13}-(\sin\theta^+\cos\theta^-)P_{31}][(\cos\theta^+\cos\theta^-)P_{11}+(\sin\theta^+\sin\theta^-)P_{21}]}{\epsilon_1{}^+-\epsilon_1{}^-}-\frac{4\sqrt{2}[(\cos\theta^+\cos\theta^-)P_{13}+(\sin\theta^+\sin\theta^-)P_{31}][(\cos\theta^+\sin\theta^-)P_{11}-(\sin\theta^+\cos\theta^-)P_{21}]}{\epsilon_1{}^+-\epsilon_2{}^-}\right\},$$

$$g_{62+}{}^l=2(\sin^2\theta^+-\cos^2\theta^+)+\frac{1}{2m_0}\left\{\frac{4[(\cos\theta^+\cos\theta^-)P_{31}+(\sin\theta^+\sin\theta^-)P_{13}]^2}{\epsilon_2{}^+-\epsilon_1{}^-}+\frac{4[(\cos\theta^+\sin\theta^-)P_{31}-(\sin\theta^+\cos\theta^-)P_{13}]^2}{\epsilon_2{}^+-\epsilon_2{}^-}-\frac{8[(\sin^2\theta^+)P_{13}{}^2/2+(\cos^2\theta^+)P_{22}{}^2]}{\epsilon_2{}^+-\epsilon_3{}^-}\right\},$$

$$g_{62+}{}^t=-2\sin^2\theta^+-\frac{1}{2m_0}\left\{\frac{4\sqrt{2}[(\cos\theta^+\cos\theta^-)P_{31}+(\sin\theta^+\sin\theta^-)P_{13}][(\cos\theta^+\sin\theta^-)P_{21}-(\sin\theta^+\cos\theta^-)P_{11}]}{\epsilon_2{}^+-\epsilon_1{}^-}-\frac{4\sqrt{2}[(\cos\theta^+\sin\theta^-)P_{31}-(\sin\theta^+\cos\theta^-)P_{13}][(\cos\theta^+\cos\theta^-)P_{21}+(\sin\theta^+\sin\theta^-)P_{11}]}{\epsilon_2{}^+-\epsilon_2{}^-}\right\},$$

$$|g_{4,5+}{}^l|=\left|2+\frac{4}{m_0}\left\{\frac{[(\cos\theta^-)P_{31}/\sqrt{2}+i(\sin\theta^-)P_{22}]^2}{\epsilon_3{}^+-\epsilon_1{}^-}+\frac{[(\sin\theta^-)P_{31}/\sqrt{2}-i(\cos\theta^-)P_{22}]^2}{\epsilon_3{}^+-\epsilon_2{}^-}\right\}\right|,$$

$$g_{4,5+}{}^t=0,$$

TABLE IV. (*continued*).

$\langle g$ Factor$\rangle$

$$g_{61-}{}^{l}=2(\cos^2\theta^- -\sin^2\theta^-)+\frac{1}{2m_0}\left\{\frac{4[(\cos\theta^+\sin\theta^-)P_{13}-(\sin\theta^+\cos\theta^-)P_{31}]^2}{\epsilon_1{}^- -\epsilon_1{}^+}+\frac{4[(\cos\theta^+\cos\theta^-)P_{31}+(\sin\theta^+\sin\theta^-)P_{13}]^2}{\epsilon_1{}^- -\epsilon_2{}^+}\right.$$
$$\left.-\frac{8[(\cos^2\theta^-)P_{31}{}^2/2+(\sin^2\theta^-)P_{22}{}^2]}{\epsilon_1{}^- -\epsilon_3{}^+}\right\},$$

$$g_{61-}{}^{t}=+2\cos^2\theta^-+\frac{1}{2m_0}\left\{\frac{4\sqrt{2}[(\cos\theta^+\sin\theta^-)P_{13}-(\sin\theta^+\cos\theta^-)P_{31}][(\cos\theta^+\cos\theta^-)P_{11}+(\sin\theta^+\sin\theta^-)P_{21}]}{\epsilon_1{}^- -\epsilon_1{}^+}\right.$$
$$\left.-\frac{4\sqrt{2}[(\cos\theta^+\cos\theta^-)P_{31}+(\sin\theta^+\sin\theta^-)P_{13}][(\cos\theta^+\sin\theta^-)P_{21}-(\sin\theta^+\cos\theta^-)P_{11}]}{\epsilon_1{}^- -\epsilon_2{}^+}\right\},$$

$$g_{62-}{}^{l}=2(\sin^2\theta^- -\cos^2\theta^-)+\frac{1}{2m_0}\left\{\frac{4[(\cos\theta^+\cos\theta^-)P_{13}+(\sin\theta^+\sin\theta^-)P_{31}]^2}{\epsilon_2{}^- -\epsilon_1{}^+}+\frac{4[(\cos\theta^+\sin\theta^-)P_{31}-(\sin\theta^+\cos\theta^-)P_{13}]^2}{\epsilon_2{}^- -\epsilon_2{}^+}\right.$$
$$\left.-\frac{8[(\sin^2\theta^-)P_{31}{}^2/2+(\cos^2\theta^-)P_{22}{}^2]}{\epsilon_2{}^- -\epsilon_3{}^+}\right\},$$

$$g_{62-}{}^{t}=-2\sin^2\theta^-+\frac{1}{2m_0}\left\{\frac{4\sqrt{2}[(\cos\theta^+\cos\theta^-)P_{13}+(\sin\theta^+\sin\theta^-)P_{31}][(\cos\theta^+\sin\theta^-)P_{11}-(\sin\theta^+\cos\theta^-)P_{21}]}{\epsilon_2{}^- -\epsilon_1{}^+}\right.$$
$$\left.-\frac{4\sqrt{2}[(\cos\theta^+\sin\theta^-)P_{31}-(\sin\theta^+\cos\theta^-)P_{13}][(\cos\theta^+\cos\theta^-)P_{21}+(\sin\theta^+\sin\theta^-)P_{11}]}{\epsilon_2{}^- -\epsilon_2{}^+}\right\}$$

$$|g_{4,5-}{}^{l}|=\left|2+\frac{4}{m_0}\left\{\frac{[(\cos\theta^+)P_{13}/\sqrt{2}+i(\sin\theta^+)P_{22}]^2}{\epsilon_3{}^- -\epsilon_1{}^+}+\frac{[(\sin\theta^+)P_{13}/\sqrt{2}-i(\cos\theta^+)P_{22}]^2}{\epsilon_3{}^- -\epsilon_2{}^+}\right\}\right|,$$

$$g_{4,5-}{}^{t}=0.$$

follows since the $L_6{}^{\pm}$ states transform like states with total angular momentum[23] $\frac{1}{2}$ so that the nonzero matrix elements of π_X and π_Y are given by $\langle C^{1/2}|\pi_+|V^{-1/2}\rangle\neq 0$ and $\langle C^{1/2}|\pi_-|V^{-1/2}\rangle=0$.[29] If this selection rule is inserted into Eq. (2.5), then the energy of the $C^{1/2}$ state is above the $C^{-1/2}$ state, i.e., the conduction g factor is positive.[30]

It is worth treating the g factors for the $L_{62}{}^-$ and $L_{4,5}{}^+$ levels in detail, both to illustrate the procedure for obtaining g factors from Eq. (2.5), and to illustrate certain differences between the $L_6{}^{\pm}$ levels and the $L_{4,5}{}^{\pm}$ Kramers-degenerate pairs of levels.

2. *g Factors for $L_{62}{}^-$ Levels*

With a magnetic field in the $+Z$ direction, the 2×2 matrix Eq. (2.5) for the $L_{62}{}^-$ levels has the form

$$E_{2\rho;2\rho}{}^{-}(\mathbf{K})=\begin{pmatrix}[E_{20}{}^-(\mathbf{K})+(\beta H/2)g_{62-}{}^{l}] & 0\\ 0 & [E_{20}{}^-(\mathbf{K})-(\beta H/2)g_{62-}{}^{l}]\end{pmatrix}, \tag{2.6}$$

where the upper-left diagonal term is the matrix element for the $L_{62}{}^-\alpha$ state and $E_{20}{}^-(\mathbf{K})$ represents the operator equation for the orbital Landau levels given by the first two terms of Eq. (2.5). It is possible to solve this operator equation and obtain the energies of the equally spaced, orbital Landau levels.[22] This is not necessary, however, since the g factor can be determined directly from the energy difference between the Kramers pair. The full expression for $g_{62-}{}^{l}$ is given in Table IV.

In the strong s.o. limit $L_{62}{}^-\alpha=(Z\uparrow+\sqrt{2}X_+\downarrow)/\sqrt{3}$ and $L_{62}{}^-\beta=(Z\downarrow-\sqrt{2}X_-\uparrow)/\sqrt{3}$. The only nonzero matrix element of $\sigma_+=(\sigma_X+i\sigma_Y)/2$ is $\langle L_{62}{}^-\alpha|\sigma_+|L_{62}{}^-\beta\rangle$ which, by the convention stated previously, established $L_{62}{}^-\alpha$ as the "up" state. Therefore the correct equation for the longitudinal g factor for the $L_{62}{}^-$ level is given, in magnitude and sign, by the sum of terms listed in Table IV.

With a magnetic field in the $+X$ direction, the g-factor terms appear in the off-diagonal positions. The sign of the g factor for the transverse field was obtained by the procedure of diagonalizing the 2×2 matrix by the linear combinations $L_{62}{}^-\beta'=(L_{62}{}^-\alpha+L_{62}{}^-\beta)/\sqrt{2}$ and $L_{62}{}^-\alpha'=(L_{62}{}^-\alpha-L_{62}{}^-\beta)/\sqrt{2}$. The only nonzero matrix element of $\sigma_+=(\sigma_Y+i\sigma_Z)/2$ for these states is $\langle L_{62}{}^-\alpha'|\sigma_+|L_{62}{}^-\beta'\rangle$. This specifies the "up" state and thus the sign of the transverse g factor. It is worth

[29] E. Feenberg and G. E. Pake, *Notes on the Quantum Theory of Angular Momentum* (Addison-Wesley Publishing Company, Inc., Reading, Massachusetts, 1953), p. 35.

[30] The essential features of this calculation are due to J. O. Dimmock (private communication).

noting that all terms in the expression for $g_{62-}{}^{l}$ are real. The above treatment also applies to the $L_{62}{}^{+}$ and $L_{61}{}^{\pm}$ levels. Therefore the total g factors for these levels are just the algebraic sums of the contributions from the other levels with opposite parity.

3. *g Factors for $L_{4,5}{}^{+}$ Levels*

With the magnetic field in the $+Z$ direction, the 2×2 matrix Eq. (2.5) for the $L_{4,5}{}^{+}$ level has the form

$$E_{3\rho;3\rho'}{}^{+}(\mathbf{K})=\begin{pmatrix} E_{30}{}^{+}(\mathbf{K}) & (-i\beta H/2)g_{4,5+}{}^{l} \\ +i(\beta H/2)g_{4,5+}{}^{l*} & E_{30}{}^{+}(\mathbf{K}) \end{pmatrix}. \tag{2.7}$$

This differs from Eq. (2.6) for the $L_{61}{}^{+}$ levels since $g_{4,5+}{}^{l}$ (defined in Table IV) is complex. The magnitude of the g factor is given by the magnitude of the sum listed in Table IV; however, the g factor is not the algebraic sum of contributions from each of the interacting levels, as is the case for the $L_{61}{}^{\pm}$ and $L_{62}{}^{\pm}$ levels, except under conditions of weak s.o. mixing ($\sin\theta^{-}=0$). The $L_{4,5}{}^{\pm}$ levels also differ from the $L_{61}{}^{\pm}$ and $L_{62}{}^{\pm}$ levels in the form of the transverse g factor. This is zero for the $L_{4,5}{}^{\pm}$ levels since both the interband and "free-electron" contributions to the transverse g factor vanish. The interband contributions vanish because the $L_{4,5}{}^{\pm}$ levels are not coupled to any other level by both transverse and longitudinal momentum matrix elements. The "free-electron" contribution vanishes because all matrix elements of σ_X and σ_Y are zero for the $L_{4,5}{}^{\pm}$ levels. The Cohen-Blount result,[20] however, applies to all levels. The contribution to the inverse effective mass-ratio perpendicular to the field by the interaction with a given level is just half the contribution to the g factor parallel to the field by interaction with the same level. This general property of pair-wise interacting, Kramers-degenerate levels provides a useful check of the over-all results of a complex $\kappa\cdot\pi$ calculation.

Lin and Kleinman[8] give expressions for the tangential g factors for the valence and conduction bands of the lead salts which do not contain interband contributions. If s.o. mixing of levels is appreciable, as in the lead salts, then both π^{t} and π^{l} are nonzero between levels with L_6 symmetry. Thus the $\kappa\cdot\pi$ contributions to the tangential g factor do not vanish and are, in fact, given in magnitude by the Cohen-Blount[20] result $|g_i{}^{t}|=2m_0/(m_i{}^{t}m_i{}^{l})^{1/2}$.

III. BAND PARAMETERS IN LIMITING APPROXIMATIONS

The equations for the band parameters listed in Table IV are valid for any combination of energies and ordering of the six bands at the L point provided that the energy separation with respect to other levels is large compared to the spread in energy of the six levels considered. In principle, it is possible to determine the order and energies of the bands (relative to the band-gap energy) in terms of measured effective masses and g factors for all the bands. These twenty-four band parameters are completely determined by the five π matrix elements listed in Eq. (2.4) and the seven energies E_g, $\epsilon_0{}^{\pm}$, $\Delta_1{}^{\pm}$, and $\Delta_2{}^{\pm}$. [The relations between this set of undetermined parameters and the set used in Table IV are given in Eq. (2.3) and in Table I.] In practice, it is more feasible to determine energy separations and relative order of the bands by other methods, insofar as possible, and use the measured band parameters to test the consistency of the assignments and calculate the unknown momentum matrix elements. The number of these unknown matrix elements can be further reduced by going to one of the limiting approximations which relates the set of levels in the real crystal to a more highly degenerate set of levels in a counterpart crystal with higher symmetry. This procedure for determining the parentage of the states has already been invoked in Sec. II B, where the eigenfunctions of the Hamiltonian [Eq. (2.1)] were related to the parent functions obtained by neglecting the s.o. term. Proceeding further in the reduction of Eq. (2.1), the potential $V(\mathbf{r})$ may be altered judiciously to yield simplified solutions and the perturbed $V(\mathbf{r})$ then treated in a manner analogous to the s.o. term.

The π matrix elements listed in Eq. (2.4) are defined in terms of the single-group symmetry functions, i.e., the s.o. mixing of the states is neglected. The relativistic contributions to π are negligible for all semiconductors so far considered; in PbTe they contribute less than 1%.[15] The limiting approximations, discussed below, introduce relations among the $\mathbf{p}$ matrix elements. The "internal" s.o. contribution to the π matrix element has been neglected. The s.o. mixing of the levels, however, is taken into account in the calculation of the band parameters.

A. Free-Electron Approximation

In this approximation, the potential $V(\mathbf{r})$ is taken to be constant. The Bloch functions are then plane waves with wave vectors given by the points of the reciprocal lattice. The six plane-wave functions $\exp[i\mathbf{k}_j\cdot\mathbf{r}]$ [where $\mathbf{k}_j=+(\pi/a_0)[\bar{1}\bar{1}3]$ and cyclic permutations] are degenerate.[11] The L-point symmetry functions can be expressed as linear combinations of these plane-wave functions and the corresponding momentum-matrix elements can thus be expressed in terms of a single matrix element for the plane-wave states. Dimmock and Wright[11] have calculated these matrix elements in the limit of weak s.o. interaction [Eqs. (3) and (4)]. The correspondence between their elements α, β, etc., and our matrix elements P_{11}, P_{13}, etc., was obtained by equating the $\mathbf{k}\cdot\mathbf{p}$ terms given in Table V of Dimmock and Wright[11] with the corresponding terms given in Table III of this work. The results are listed in Table V in terms of the single matrix element P_0 which is left as an undetermined parameter. The magnitude of P_0

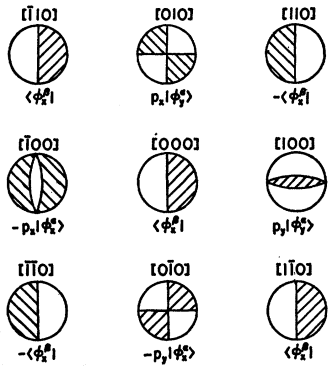

FIG. 1. Schematic representation of the four nonzero momentum matrix elements for the nearest-neighbor interaction of a φ_x^β cation p orbital located at the lattice site $[000]a_0/2$ with the appropriate φ_i^α p orbital located at one of the adjacent anion sites. The tight-binding approximation case (a) includes only the contributions of the form $\langle\varphi_x^\beta|p_x|\varphi_x^\alpha\rangle$ while case (b) includes contributions of the form $\langle\varphi_x^\beta|p_y|\varphi_y^\alpha\rangle$ as well. At the Γ point a contribution such as that from the orbital located on the $[100]a_0/2$ lattice site is cancelled by the contribution from the orbital located on the $[\bar{1}00]a_0/2$ lattice site. At the L point, the phase factor differs by (-1) for alternate atomic layers in the $\langle 111\rangle$ direction so that the contributions from inverse lattice sites are additive.

can be estimated from the relation $P_0=\hbar\pi/a_0\sqrt{3}$, where a_0 is the lattice constant.[11] The number of π matrix elements is reduced from five to one in this approximation. Although the "free-electron" limit gives the correct set of symmetry states at L, it does not adequately approximate the lead salts inasmuch as it predicts bands of the order 8 eV wide[11] along the Λ axis while the values calculated by more sophisticated techniques are of the order of 3 eV.[7,8] This suggests that some form of tight-binding approximation would provide a better starting approximation.

B. Tight-Binding Approximation

In the tight-binding approximation the Bloch functions are chosen as linear combinations of atomic orbitals centered on the lattice sites of the crystal.[31] The Bloch functions can be written in the form

$$\Psi_i(\mathbf{k},\mathbf{r})=\sum_j\sum_l\sum_p e^{i\mathbf{k}\cdot(\mathbf{r}_l+\mathbf{r}_p)}[a_{ij}{}^p\varphi_j{}^p(\mathbf{r}-\mathbf{r}_l-\mathbf{r}_p)], \quad (3.1)$$

where the $\varphi_j{}^p(\mathbf{r}-\mathbf{r}_l-\mathbf{r}_p)$ are suitably orthogonalized atomic wave functions[31] positioned on the lattice sites $\mathbf{r}_l+\mathbf{r}_p$. Here $\mathbf{r}_l$ are the translation vectors of the lattice and $\mathbf{r}_p$ are the position vectors of the atoms of different kind within the unit cell. The expansion coefficients are represented by $a_{ij}{}^p$. The upper three valence bands and lower three conduction bands in the lead salts are relatively flat along the Λ axis,[7,8] and are quite well separated in energy from other bands. A natural choice for the tight-binding origin of these six bands is the three spin-degenerate p orbitals associated with the anion sites (S, Se, or Te) and the three p orbitals associated with the cation sites (Pb). A pair of lower valence bands, not considered here, would then be associated with the anion and cation s orbitals.

An interesting feature of the bands formed from anion and cation p orbitals in the NaCl lattice is that the two sets are decoupled at the L point, i.e., neglecting relativistic effects, the valence bands can be expressed in terms of p orbitals associated with one of the sublattices and the conduction bands with p orbitals on the other sublattice. Referred to a common origin, one set of bands at L is even and the other set odd, so that the interband matrix elements of the momentum $\mathbf{p}$ are allowed. At Γ, on the other hand, the p orbitals on the sublattices are not decoupled. Furthermore, both the valence bands and the conduction bands derived from these p orbitals are odd so that the corresponding interband $\mathbf{p}$ matrix elements are zero.

The nonzero matrix elements of the Hamiltonian for the simple cubic lattice have been obtained by Slater and Koster[31] in the tight-binding approximation for first- and second-nearest-neighbor interactions. The corresponding matrix elements for the NaCl lattice can be selected from their listing and utilized to form appropriate linear combinations of orbitals for various points in the Brillouin zone. This restriction to nearest- and next-nearest-neighbor overlap is not necessary in the present case since the appropriate combinations of anion and cation p orbitals at the Γ point and L point can be simply obtained by symmetry alone (see Appendix).

The matrix elements of the momentum $\mathbf{p}$ can be reduced to terms of the form $\langle\sum_\alpha e^{-i\mathbf{k}_0\cdot\mathbf{r}_\alpha}\varphi_i{}^\beta(\mathbf{r}-\mathbf{r}_\alpha)|\times p_j|\varphi_k{}^\beta(\mathbf{r})\rangle$, where, as before, i, j, and k are Cartesian labels. The symmetry-allowed matrix elements are shown schematically in Fig. 1 for the special case of nearest-neighbor interactions only. The only matrix elements which are expected to survive in the extreme tight-binding limit are those of the form $\langle\varphi_x{}^\beta(\mathbf{r}-\mathbf{r}_0)|\times p_x|\varphi_x{}^\beta(\mathbf{r})\rangle$, where $\mathbf{r}_0$ is the displacement of a nearest-

TABLE V. The π matrix elements given by Eqs. (2.4) are calculated in a "free-electron" and two "tight-binding" approximations described in the text. The nonzero matrix elements for the tight-binding cases (a) and (b) are shown schematically in Fig. 1. In terms of these matrix elements case (b) corresponds to

$$P_a'=N\{\langle\varphi_x{}^\beta|p_x|\varphi_x{}^\alpha\rangle+2\langle\varphi_x{}^\beta|p_y|\varphi_y{}^\alpha\rangle\}$$

and

$$P_b'=N\{\langle\varphi_x{}^\beta|p_x|\varphi_x{}^\alpha\rangle-\langle\varphi_x{}^\beta|p_y|\varphi_y{}^\alpha\rangle\},$$

where N is a normalizing factor. Case (a) corresponds to the neglect of the second term in the above expressions.

	Free-electron limit	Tight-binding limit (a)	Tight-binding limit (b)
P_{11}	P_0	P_a	P_a'
P_{13}	$4P_0$	P_a	P_a'
P_{31}	$4P_0$	P_a	P_b'
P_{21}	P_0	P_a	P_b'
P_{22}	$2\sqrt{2}P_0$	$-P_a/\sqrt{2}$	$-P_b'/\sqrt{2}$

[31] J. C. Slater and G. F. Koster, Phys. Rev. 94, 1498 (1954).

neighbor sulfur site relative to a lead site. In this approximation, the π matrix elements defined by Eq. (2.4) can be readily evaluated in terms of the tight-binding functions of the Appendix. These matrix elements are listed as case (a) in Table V in terms of the single parameter P_a. Another useful approximation is obtained by including matrix elements of the form $\langle\varphi_x^\alpha(\mathbf{r}-\mathbf{r}_0)|p_y|\varphi_y^\beta(\mathbf{r})\rangle$. The corresponding matrix elements are listed in Table V as tight-binding case (b).

C. Spherical Approximation

The limiting approximations developed in the preceding sections allow considerable simplification of the equations for the g factors and effective masses listed in Table IV. The "nearly-free-electron" approximation and the "extreme tight-binding" approximation case (a) reduce the number of undetermined parameters to a single-momentum matrix element, provided the energies of the levels are determined. The "nearly-free-electron" approximation, however, does not appear appropriate for the lead salts, although it may apply to other materials. The "tight-binding" approximations (a) and (b) appear to be more satisfactory starting points for the lead salts. These approximations lead to spherical effective masses and g factors for the L_{61}^+ and L_{62}^- levels under conditions which are appropriate for PbS. The observed g factors and effective masses of the valence and conduction bands are likewise nearly spherical for PbS.[12–14]

The nearly spherical valence and conduction bands in PbS have, in the past, led to the mistaken assignment of the Γ point for the band extrema. This was a natural mistake since, if the spin-orbit mixing of bands of the same symmetry is ignored, then the $\mathbf{k}\cdot\mathbf{p}$ coupling between any pair of bands at the L point is either longitudinal or transverse but not both. Spherical bands at L are therefore unlikely, without large spin-orbit interaction, since the longitudinal interaction with one band would have to be balanced by the transverse interaction with at least one other band lying at another energy. To have just such a balance for both the valence band and conduction band would thus appear to be an extreme coincidence. When s.o. mixing of bands is included, however, both the longitudinal and transverse momentum matrix elements are coupled between bands with L_6 symmetry and opposite parity.

The odd (−) levels at L in PbS are p like around the lead site and s or d like around the sulfur site.[7,11] In the tight-binding limit, these bands originate from the lead p orbitals. Large s.o. mixing of these levels is expected since the s.o. splitting of the $6p$ levels in atomic lead is quite large (1.4 eV).[32] The s.o. splitting in the crystal depends on the relative contributions from the lead core and from the sulfur core and is reduced somewhat since the s.o. contribution from the sulfur is small. Dimmock and Wright[11] give an estimate of 0.96 eV for s.o. splitting in the crystal assuming the electrons spend 40% of the time on the lead atom and 60% on the sulfur atom. This proportion holds fairly well for the covalent III-V compounds but is not expected to be too accurate for the ionic lead salts. In the tight-binding limit the s.o. splitting of the conduction band at L would be the same as for atomic lead (1.4 eV).

The even (+) states at L are s- or d-like around the lead site and p like around the sulfur site. In the tight-binding limit these bands originate from the sulfur p orbitals. The s.o. splittings of the lead d orbitals and sulfur p orbitals are both of the order of 0.06 eV and are thus negligible. The $L_6^+(L_1)$ level may have s-like and/or d-like character around the lead atom. Strong s character would affect the energy of this level but would not necessarily introduce strong mixing with the d-like $L_6^+(L_3)$ level.

The identification of the odd states as conduction levels and even states as valence levels, without specifying the internal ordering, follows the previous work.[7,8,11] This assignment is supported for PbS by the fact that the L_{62}^- level lies lower in energy than the L_{61}^-, $L_{4,5}^-$ pairs of levels for lead p orbitals. The s.o. splitting has the same sign as in the valence band of germanium and the III-V compounds. This leaves the L_{61}^+ level as the valence band with the closely spaced L_{62}^+, $L_{4,5}^+$ pair of levels at some lower energy. Also, L_6 symmetry with opposite parity is specified for the valence- and conduction-band edges in order to have nearly spherical effective masses.

With this ordering of levels, the g factors and effective masses in the spherical approximation were calculated from the equations listed in Table IV with the matrix elements given by case (b) in Table V. For the valence (L_{61}^+) and conduction (L_{62}^-) bands we obtain

$$(m_v{}^l)^{-1}=(m_v{}^t)^{-1}=(m_0)^{-1}\left\{1-\frac{4}{3}\left(\frac{\lambda_c+3}{\lambda_c+1}\right)\frac{P_a{}'^2}{2m_0E_g}\right\},$$

$$(m_c{}^l)^{-1}=(m_c{}^t)^{-1}=(m_0)^{-1}\left\{1+\frac{4}{3}\left(\frac{\lambda_v+2\gamma+1}{\lambda_v+1}\right)\times\frac{P_a{}'^2}{2m_0E_g}\right\}, \quad (3.2)$$

$$g_v{}^l=g_v{}^t=g_0\left\{1-\frac{4}{3}\left(\frac{\lambda_c}{\lambda_c+1}\right)\frac{P_a{}'^2}{2m_0E_g}\right\},$$

$$g_c{}^l=g_c{}^t=-g_0\left\{\frac{1}{3}-\frac{4}{3}\left(\frac{\lambda_v+1-\gamma}{\lambda_v+1}\right)\frac{P_a{}'^2}{2m_0E_g}\right\},$$

where λ_c is the ratio of the energy separation between L_{61}^- and L_{62}^- to the energy gap E_g. Similarly, λ_v is the ratio of the valence-band splitting $L_{61}^+-L_{62}^+$ to E_g

[32] F. Herman and S. Skillman, *Atomic Structure Calculations* (Prentice-Hall, Inc., Englewood Cliffs, New Jersey, 1963).

and γ is the ratio of the parameters $P_a'^2/P_b'^2$. In the extreme tight-binding limit case (a) this ratio is 1. It is worth noting that the contributions to the effective masses and g factors from the valence–conduction-band interaction are spherical in this approximation. The contributions from the more distant bands are likewise spherical. Lin and Kleinman[8] obtained a different composition for the conduction band and a different set of matrix elements which give a spherical valence-conduction-band effective-mass contribution. The contributions from the higher bands, however, are not spherical. Their quoted g factors are highly nonspherical since the interband contributions to the tangential g factor were neglected.

As might be expected, the equation for the effective masses and g factors of the s-like valence band are the same, in the tight-binding limit, as for the s-like conduction band at Γ in germanium.[33] The correspondence with Eqs. (A4) of Ref. 33 is obtained by the substitution $\mathcal{E}_g=-E_g(1+\lambda_c)$ and $\Delta=\lambda_c E_g$, which relate the ordering of bands to that given here.

D. Nonparabolicity

The parabolic approximation to the band parameters is only valid over a range of energies into a given band which is small compared to the energy interval to the nearest band with allowed $\boldsymbol{\kappa}\cdot\mathbf{p}$ interaction. The range of validity may be extended by expanding the energies in powers of the wave vector $\boldsymbol{\kappa}$; however, this method also fails when the $\boldsymbol{\kappa}\cdot\mathbf{p}$ energy for any pair of bands exceeds their energy separation at $\mathbf{k}_0$.

An alternative procedure has been used by Kane[16] to further extend the range of validity in the absence of an external magnetic field. The solution proceeds in two stages. First the $\mathbf{k}\cdot\mathbf{p}$ interaction between "weakly" interacting bands is removed by a perturbation treatment such as the power series expansion in $\boldsymbol{\kappa}$. The resulting Hamiltonian with renormalized matrix elements is then solved exactly. This procedure has very definite advantages since it is still valid in the range where the series expansion in $\boldsymbol{\kappa}$ diverges. Also, the number of "strongly" interacting bands is usually quite small; e.g., in the lead salts the $\mathbf{k}\cdot\mathbf{p}$ energies for all bands of the initial set, except the valence-conduction band pair, are less than the corresponding energy gaps throughout most of the zone. Only the remaining pair of renormalized bands needs to be treated in detail.

The eigenfunctions for the Hamiltonian [Eq. (2.5)] in the presence of a magnetic field are products of the Bloch functions times harmonic-oscillator functions F_n.[22] The raising and lowering operators acting on the oscillator functions are obtained from the commutator relation $[\mathrm{K}_i,\mathrm{K}_j]=is\epsilon_{ijk}\lambda^k$.[22] The quantities are defined in Sec. II E. For a magnetic field in the Z direction, $\mathrm{K}_\pm=(\mathrm{K}_X\pm i\mathrm{K}_Y)/\sqrt{2}$; $\mathrm{K}_+F_n=[(n+1)s]^{1/2}F_{n+1}$; and $\mathrm{K}_-F_n=(ns)^{1/2}F_{n-1}$. The valence–conduction-band Hamiltonian with renormalized parameters is given by the matrix

	$C^{1/2}F_n$	$V^{-1/2}F_{n+1}$	$C^{-1/2}F_{n+1}$	$V^{1/2}F_n$
$C^{1/2}F_n$	$\frac{E_g}{2}+(n+\frac{1}{2})\hbar\tilde{\omega}_c{}^l+\bar{g}_c{}^l\frac{\beta H}{2}$	$[E_g(n+1)\hbar\tilde{\omega}_{vc}{}^l]^{1/2}$	0	$\hbar\kappa_z[E_g/2\tilde{m}_{vc}{}^l]^{1/2}$
$V^{-1/2}F_{n+1}$	$[E_g(n+1)\hbar\tilde{\omega}_{vc}{}^l]^{1/2}$	$-\frac{E_g}{2}+(n+\frac{3}{2})\hbar\tilde{\omega}_v{}^l-\bar{g}_v{}^l\frac{\beta H}{2}$	$\hbar\kappa_z[E_g/2\tilde{m}_{vc}{}^l]^{1/2}$	0
$C^{-1/2}F_{n+1}$	0	$\hbar\kappa_z[E_g/2\tilde{m}_{vc}{}^l]^{1/2}$	$\frac{E_g}{2}+(n+\frac{3}{2})\hbar\tilde{\omega}_c{}^l-\bar{g}_c{}^l\frac{\beta H}{2}$	$[E_g(n+1)\hbar\tilde{\omega}_{vc}{}^l]^{1/2}$
$V^{1/2}F_n$	$\hbar\kappa_z[E_g/2\tilde{m}_{vc}{}^l]^{1/2}$	0	$[E_g(n+1)\hbar\tilde{\omega}_{vc}{}^l]^{1/2}$	$-\frac{E_g}{2}+(n+\frac{1}{2})\hbar\tilde{\omega}_c{}^l+\bar{g}_v{}^l\frac{\beta H}{2}$

(3.3)

where $C^{\pm1/2}$ and $V^{\pm1/2}$ represent the renormalized conduction- and valence-band functions with the "weak" interactions removed to lowest order. The longitudinal cyclotron energies are given by $\hbar\omega^l=2\beta H(m^t)^{-1}$, where the masses for the barred energies are given by the equations in Table IV with the valence-conduction band term deleted. Similarly, the barred g factors are obtained from Table IV with the valence-conduction term deleted. The energy $\hbar\tilde{\omega}_{vc}{}^l$ is obtained with the mass term given by the valence-conduction band interaction. For convenience, the zero-in-energy has been taken at the middle of the energy gap.

The energies of the levels at $\kappa_z=0$ are obtained by diagonalizing the decoupling 2×2 matrix equations

$$E_{Cn\pm}=\tfrac{1}{2}\{(n+\tfrac{1}{2})(\hbar\tilde{\omega}_c{}^l+\hbar\tilde{\omega}_v{}^l)\pm[(\bar{g}_c{}^l-\bar{g}_v{}^l)\beta H/2+\hbar\tilde{\omega}_v{}^l]\}$$
$$+(E_g/2)^{1/2}\{[E_g/2+(n+\tfrac{1}{2})(\hbar\omega_c{}^l-\hbar\omega_v{}^l)]$$
$$\pm[(g_c{}^l+g_v{}^l)\beta H/2-\hbar\omega_v{}^l]\}^{1/2},$$

[33] L. M. Roth, B. Lax, and S. Zwerdling, Phys. Rev. 114, 90 (1959).

$$E_{Vn\pm}=\tfrac{1}{2}\{(n+\tfrac{1}{2})(\hbar\bar{\omega}_c{}^l+\hbar\bar{\omega}_v{}^l)\mp[(\bar{g}_c{}^l-\bar{g}_v{}^l)\beta H/2-\hbar\bar{\omega}_c{}^l]\}$$
$$-(E_g/2)^{1/2}\{[E_g/2+(n+\tfrac{1}{2})(\hbar\omega_c{}^l-\hbar\omega_v{}^l)]$$
$$\mp[(g_c{}^l+g_v{}^l)\beta H/2-\hbar\omega_c{}^l]\}^{1/2}, \quad (3.4)$$

where the energy labels refer to the nth Landau level for the $\pm\frac{1}{2}$ state of the conduction and valence band. In the process of regrouping terms within the square root we have neglected quantities of the order $[(n+\frac{1}{2})(\hbar\bar{\omega}_c{}^l-\hbar\bar{\omega}_v{}^l)/E_g]^2$.

The low-field nonparabolic effective masses M_i and g factors G_i may be obtained from Eqs. (3.4) in simplified form by defining the effective mass in terms of the Landau spacing dE_n/dn and the g factor in terms of the energy difference $(E_{n+}-E_{n-})$.

$$(M_c{}^l)^{-1}=\frac{1}{2}\left\{(\bar{m}_c{}^l)^{-1}+(\bar{m}_v{}^l)^{-1}\right.$$
$$\left.+\frac{[(m_c{}^l)^{-1}-(m_v{}^l)^{-1}]}{[1+2(n+\frac{1}{2})(\hbar\omega_c{}^l-\hbar\omega_v{}^l)/E_g]^{1/2}}\right\},$$
$$G_c{}^l=\frac{1}{2}\left\{(\bar{g}_c{}^l-\bar{g}_v{}^l)+2(\bar{m}_v{}^l/m_0)^{-1}\right. \quad (3.5)$$
$$\left.+\frac{[(g_c{}^l+g_v{}^l)-2(m_v{}^l/m_0)^{-1}]}{[1+2(n+\frac{1}{2})(\hbar\omega_c{}^l-\hbar\omega_v{}^l)/E_g]^{1/2}}\right\},$$

with similar equations for the valence band. In Eqs. (3.4) and (3.5), the lower case unbarred and barred parameters are the values determined in the parabolic approximation, with and without the valence-conduction band term. It is to be recalled that the signs refer to electronic states, i.e., $m_v{}^l$ is generally negative. Thus the energy ratio responsible for the nonparabolicity is the ratio of the sum of Landau energies in valence and conduction band to half the gap. The expressions for the nonparabolic parameters reduce to the parabolic form in the low-field limit.

IV. CONCLUSIONS

The $\mathbf{k}\cdot\mathbf{p}$ and s.o. interactions among a set of six levels at the L point for the NaCl lattice have been treated in detail. The set chosen is obtained from anion and cation p orbitals in the tight-binding limit and is the same set adopted in the previous work. The double-group basis functions derived here, however, differ from those published previously. We have verified our choice by group theory and also by obtaining a correspondence, in the limit of large s.o. interaction, with the basis functions for bands at the Γ point derived from p orbitals in the group IV elements and III-V compounds. In some of the published work, the spin assignments in the basis functions were reversed which leads to incorrect signs for the g factors. We discuss the sign convention for the g factor in order to resolve any ambiguity in sign and to provide a test for future work.

The s.o. coupling in the lead salts is large which leads to appreciable mixing of levels with the same double-group symmetry. This in turn allows both the longitudinal and transverse coupling of the π matrix element between levels with $L_6{}^+$ and $L_6{}^-$ symmetry so that spherical, or nearly spherical bands may result from the $\mathbf{k}\cdot\boldsymbol{\pi}$ interaction of a single pair of levels. The general $\mathbf{k}\cdot\boldsymbol{\pi}$ matrix elements, among the set of six levels, were obtained in terms of two mixing parameters and five momentum matrix elements. The general expressions for the parabolic effective masses and g factors for the six bands were then obtained in terms of these parameters. Expressions for the nonparabolic effective mass and g-factor parameters, valid over an extended range, were obtained under the approximation, appropriate for the lead salts, that all bands except one interact weakly with the band of interest. These results extend and correct prior work and provide a basis for detailed interpretation of the magneto-optical experiments on the lead salts.

The tight-binding limit for bands derived from anion and cation p orbitals was investigated in detail since this model gives direct insight into the physical origin of nearly spherical valence- and conduction-band extrema at the I point of the Brillouin zone. These features of the band structure of PbS, which have been a puzzle in the past, follow naturally from the model. In this model for PbS, the nonzero $\mathbf{k}\cdot\mathbf{p}$ perturbation between the valence and conduction bands at the L point leads to relative maxima for the valence bands and relative minima for the conduction bands. At the Γ point, on the other hand, the $\mathbf{k}\cdot\mathbf{p}$ perturbation is zero. The spherical conduction and valence bands result from the large s.o. mixing of the conduction bands derived from lead p orbitals. In the large s.o. limit, these bands are similar in detail to the valence bands at Γ in germanium and InSb. The valence band of PbS at the L point corresponds to the conduction band of InSb at the Γ point and the conduction band of PbS at L corresponds to the split-off valence band of InSb at Γ.

ACKNOWLEDGMENTS

The authors wish to thank J. O. Dimmock for his many comments and suggestions. We thank G. W. Pratt, Jr., C. D. Kuglin, P. J. Lin, and L. Kleinman for preprints of their work and for helpful correspondence. We thank B. D. McCombe for checking the tight-binding calculations and calling our attention to recent work on bismuth.

APPENDIX: TIGHT-BINDING MOMENTUM MATRIX ELEMENTS

A. Selection Rules at Γ

We choose for a basis the Bloch functions

$$\Psi_j{}^\rho(\mathbf{k},\mathbf{r})=\sum_\rho e^{i\mathbf{k}\cdot\mathbf{r}_\rho}\varphi_j{}^\rho(\mathbf{r}-\mathbf{r}_\rho), \quad (A1)$$

where the label ρ refers separately to either a sum of orbitals associated with the anion sublattice sites located by the position vectors $\mathbf{r}_\alpha$ or to the sum of another set of orbitals located at the cation sites $\mathbf{r}_\beta$. The functions $\varphi_i{}^\rho(\mathbf{r}-\mathbf{r}_\rho)$ are p orbitals which transform like $x[100]$, $y[010]$, and $z[001]$ about the lattice site $\mathbf{r}_\rho$. At the Γ point ($\mathbf{k}=0$), $\Psi_i{}^\alpha(0,\mathbf{r})$, and $\Psi_i{}^\beta(0,\mathbf{r})$ likewise transform like x, y, $z(\Gamma_4^-)$ since the phase factor in the sum is zero. The diagonal matrix elements of the Hamiltonian (neglecting s.o.) with respect to the $\Psi_i{}^\alpha(0,\mathbf{r})$ functions have a single value which can be represented by the parameter $E_0{}^\alpha$. Similarly, the diagonal elements for the $\Psi_j{}^\beta(0,\mathbf{r})$ functions are given by $E_0{}^\beta$. The nondiagonal matrix elements $\langle\Psi_i{}^\alpha(0,\mathbf{r})|\times H|\Psi_j{}^\alpha(0,\mathbf{r})\rangle$ and $\langle\Psi_i{}^\alpha(0,\mathbf{r})|H|\Psi_j{}^\beta(0,\mathbf{r})\rangle$ are zero for $i\neq j$. These matrix elements can be reduced to terms of the form $\langle\varphi_i{}^\alpha(0,\mathbf{r})|H|\sum_\alpha\varphi_j{}^\alpha(\mathbf{r}-\mathbf{r}_\alpha)\rangle$ or $\langle\varphi^\alpha(\mathbf{r})|\times H|\sum_\beta\varphi_j{}^\beta(\mathbf{r}-\mathbf{r}_\beta)\rangle$, where the origin is chosen at one of the equivalent anion sites. This matrix element goes into the negative of itself under a coordinate rotation of π about the i axis. This operation is a member of the group of Γ and therefore the matrix elements are zero. Thus the only nondiagonal matrix elements of the Hamiltonian at Γ are $\langle\Psi_i{}^\alpha(0,\mathbf{r})|H|\Psi_i{}^\beta(0,\mathbf{r})\rangle=E_0{}^{\alpha\beta}$. The tight-binding valence and conduction bands at Γ are therefore given by

$$\begin{aligned}X_i(\Gamma)&=\sin\gamma\Psi_i{}^\alpha(0,\mathbf{r})-\cos\gamma\Psi_i{}^\beta(0,\mathbf{r}),\\ X_i'(\Gamma)&=\cos\gamma\Psi_i{}^\alpha(0,\mathbf{r})+\sin\gamma\Psi_i{}^\beta(0,\mathbf{r}),\end{aligned}\tag{A2}$$

where $\tan2\gamma=2E_0{}^{\alpha\beta}(E_0{}^\alpha-E_0{}^\beta)^{-1}$. Both sets of functions are odd about either the α or β sites so that the matrix elements of the momentum $\mathbf{p}$ are all zero.

B. Selection Rules at L

At the L point the diagonal matrix elements of the Hamiltonian are given by the parameters $E_L{}^\alpha$ and $E_L{}^\beta$, which can be related to the parameters at Γ if only nearest-neighbor or next-nearest-neighbor interactions are considered. The nondiagonal matrix elements $\langle\Psi_i{}^\alpha(\mathbf{k}_0,\mathbf{r})|H|\Psi_j{}^\beta(\mathbf{k}_0,\mathbf{r})\rangle$ vanish. These matrix elements can be reduced to sums of terms which are equal to $\langle\sum_\alpha e^{-i\mathbf{k}_0\cdot\mathbf{r}_\alpha}\varphi_i{}^\alpha(\mathbf{r}-\mathbf{r}_\alpha)|H|\varphi_j{}^\beta(\mathbf{r})\rangle$, where the origin of the coordinate system is chosen at one of the lead sites $\mathbf{r}_\beta$. The inversion operator ($J\mathbf{r}\rightarrow-\mathbf{r}$) is a member of the group at L. Applying the inversion operator and also reversing the sign of the lattice vectors which are summed over ($\mathbf{r}_\alpha\rightarrow-\mathbf{r}_\alpha'$) the coupling terms can be rewritten $\langle\sum_{\alpha'}e^{i\mathbf{k}_0\cdot\mathbf{r}_{\alpha'}}\varphi_i{}^\alpha(\mathbf{r}-\mathbf{r}_\alpha')|H|\varphi_j{}^\beta(\mathbf{r})\rangle$ which formally differs from the original only by the multiplicative factor $\exp(i2\mathbf{k}_0\cdot\mathbf{r}_\alpha')$. The position vectors of the anion sites relative to one of the lead sites can be written as a lattice vector $\mathbf{r}_l$ of the lead sublattice plus the displacement $\mathbf{r}_0$ of the anion sublattice relative to the lead sublattice ($\mathbf{r}_\alpha'=\mathbf{r}_l+\mathbf{r}_0$) since $2\mathbf{k}_0$ is a vector of the reciprocal lattice and $\mathbf{r}_l$ a vector of the real lattice [$\exp(i2\mathbf{k}_0\cdot\mathbf{r}_l)=1$]. However, $\exp(i2\mathbf{k}_0\cdot\mathbf{r}_0)=-1$, so that the matrix element reverses sign under the described operation and is therefore zero. This result also follows from the observation that L-point Bloch functions have a periodicity of twice the lattice spacing in the [111] direction so that relative to a given lead site, the orbitals located at $\pm\mathbf{r}_\alpha$ have opposite sign.

The only nonzero off-diagonal matrix elements of the Hamiltonian are of the form $\langle\Psi_i{}^\alpha(\mathbf{k}_0,\mathbf{r})|H|\Psi_j{}^\alpha(\mathbf{k}_0,\mathbf{r})\rangle$ which are equal, apart from a constant factor, to the matrix elements $\langle\varphi_i{}^\alpha(r)|H|\sum_l e^{i\mathbf{k}_0\cdot\mathbf{r}_l}\varphi_j{}^\alpha(\mathbf{r}-\mathbf{r}_l)\rangle$, where the origin is at one of the α sites. The three matrix elements are equal for a given sublattice and may be represented by the parameters $E_L{}^{\alpha\alpha}$ and $E_L{}^{\beta\beta}$. The appropriate linear combinations which diagonalize the truncated Hamiltonian at L are

$$\begin{aligned}X^\rho(L)&=(6)^{-1/2}\sum_\rho e^{i\mathbf{k}_0\cdot\mathbf{r}_\rho}[2\varphi_z{}^\rho(\mathbf{r}-\mathbf{r}_\rho)-\varphi_x{}^\rho(\mathbf{r}-\mathbf{r}_\rho)\\&\qquad-\varphi_y{}^\rho(\mathbf{r}-\mathbf{r}_\rho)],\\ Y^\rho(L)&=(2)^{-1/2}\sum_\rho e^{i\mathbf{k}_0\cdot\mathbf{r}_\rho}[\varphi_x{}^\rho(\mathbf{r}-\mathbf{r}_\rho)-\varphi_y{}^\rho(\mathbf{r}-\mathbf{r}_\rho)],\\ Z^\rho(L)&=(3)^{-1/2}\sum_\rho e^{i\mathbf{k}_0\cdot\mathbf{r}_\rho}[\varphi_x{}^\rho(\mathbf{r}-\mathbf{r}_\rho)+\varphi_y{}^\rho(\mathbf{r}-\mathbf{r}_\rho)\\&\qquad+\varphi_z{}^\rho(\mathbf{r}-\mathbf{r}_\rho)],\end{aligned}\tag{A3}$$

where ρ refers separately to the sum over anion sites α or the sum over cation sites β. The wave vector at L is $\mathbf{k}_0=(\pi/a_0)[111]$. Each of these sets of functions is odd about an origin taken at one of its own sublattice sites. However, if a common origin at one of the β (Pb) sites is chosen, then the $X^\beta(L)$, $Y^\beta(L)$, and $Z^\beta(L)$ are odd and correspond to the L-point basis functions X, Y, and Z. Referred to the same origin, the functions $X^\alpha(L)$, $Y^\alpha(L)$, and $Z^\alpha(L)$ are even and linear combinations can be found which transform like the basis functions R and $S_\pm$. Due to an awkward convention which was adopted early in this work, the direct identification of $X^\alpha(L)$ with S_X, etc., is not valid.

Consider the transformation properties of $\Psi_i{}^\rho(\mathbf{k}_0,\mathbf{r})$ under the group of L-point symmetry operations Q.

$$\Psi_i{}^\rho(\mathbf{k}_0,Q\mathbf{r})=\sum_{\rho'}e^{i(\mathbf{k}_0+\boldsymbol{\kappa}')\cdot\mathbf{r}_{\rho'}}\varphi_i{}^\rho(Q[\mathbf{r}-\mathbf{r}_{\rho'}]),\tag{A4}$$

where $Q^{-1}\mathbf{r}_\alpha=\mathbf{r}_\alpha'$ or $Q^{-1}\mathbf{r}_\beta=\mathbf{r}_\beta'(Q^{-1}\mathbf{r}_\rho=r_\rho')$ and $Q^{-1}\mathbf{k}_0=\mathbf{k}_0+\boldsymbol{\kappa}'$ with $\boldsymbol{\kappa}'=0$ for operations which leave $\mathbf{k}_0$ invariant and $\boldsymbol{\kappa}'=2\mathbf{k}_0$ for the operations which send $\mathbf{k}_0$ into $-\mathbf{k}_0$. Since $\mathbf{r}_\beta$ and $\mathbf{r}_\beta'$ are translation vectors of the lattice which are included in the sum and $\boldsymbol{\kappa}'$ is a vector of the reciprocal lattice, the functions $\Psi_i{}^\beta(\mathbf{k}_0,r)$ transform like $\varphi_i(\mathbf{r})$, i.e., like x, y, and z in the crystal coordinate system. Thus the functions $X^\beta(L)$, $Y^\beta(L)$, and $Z^\beta(L)$ transform like X, Y, and Z in the ellipsoid coordinate system. The functions are real since the $\varphi_i(\mathbf{r})$ are real and $\exp(i\mathbf{k}_0\cdot\mathbf{r}_\beta)=\pm1$.

Similarly, it can be shown that the $\Psi_i{}^\alpha(\mathbf{k}_0,\mathbf{r})$ are pure imaginary functions which transform like x, y, and z except for a multiplicative factor of -1 under

those operations which send $\mathbf{k}_0$ into $-\mathbf{k}_0$ (i.e., J and $3C_2$). This follows since $\exp(-i2\mathbf{k}_0\cdot\mathbf{r}_\alpha)=-1$ and $\exp(i\mathbf{k}_0\cdot\mathbf{r}_\alpha)=\pm i$ when the origin is chosen at one of the β sites. Relating these transformation properties of the functions $X^\alpha(L)$, $Y^\alpha(L)$, and $Z^\alpha(L)$ to the transformation properties of R and $S_\pm$ given in Table II, we obtain

$$R=iZ_L{}^\alpha, \quad S_+=+(X_L{}^\alpha+iY_L{}^\alpha)/\sqrt{2}$$

and

$$S_-=-(X_L{}^\alpha-iY_L{}^\alpha)/\sqrt{2}.$$

PHYSICAL REVIEW VOLUME 151, NUMBER 2 11 NOVEMBER 1966

Magnetoresistance of n-Type Germanium in the Phonon-Assisted Hopping Conduction Range at High Magnetic Fields*

J. A. CHROBOCZEK† AND R. J. SLADEK
Department of Physics, Purdue University, Lafayette, Indiana
(Received 24 June 1966)

The transverse magnetoresistance ρ/ρ_0 of phonon-assisted hopping conduction in n-type germanium samples having phosphorus concentrations N_d between 5×10^{15} and 2×10^{16} cm^{-3} has been measured at 4.2°K as a function of the strength and orientation of the magnetic induction $\mathbf{B}$ in a (110) plane up to much higher values of B (78 kG) than used in previous work (30 kG). It is found that ρ/ρ_0 is an increasing function of B^2/N_d up to the highest values of B and depends on the direction of $\mathbf{B}$, the anisotropy being more complicated at higher B. For $\mathbf{B}\|[001]$, ρ/ρ_0 increases most rapidly (almost exponentially) with B. Following Sladek and Keyes these effects are explained qualitiatively in terms of the influence of the magnetic field on the donor wave functions. A simple extension of the magnetoresistance theory of Mikoshiba is made and compared with our anisotropy curves. A reasonably good fit requires that the difference in phase between wave functions on adjacent donors have a much smaller effect than expected of following Mikoshiba's method of choosing a certain parameter ϵ. A more reasonable choice of ϵ, which also includes the influence of the decrease in size of the donor wave functions due to the magnetic field, greatly reduces the calculated phase effect. A final choice of values for ϵ and a parameter relating the spacing to the concentration of impurities yields a calculated anisotropy curve which reproduces the main features of the experimental curve in remarkable detail.

MAGNETORESISTANCE of n-type Ge in the phonon-assisted hopping conduction range has been observed previously by Sladek and Keyes (SK),[1] Yamanouchi,[2] and Lee and Sladek[3] at magnetic fields up to 30 kG. The observations of SK were shown to be consistent with the theory of Mikoshiba,[4] which appeared shortly after their experiment. Our present results concern the region of higher magnetic fields, up to 78 kG. The magnitude of the magnetoresistance in this region is much larger, and the anisotropy of the effect is larger by an order of magnitude and has more complicated structure, than at lower fields. In this paper we compare our observations with the theory of Mikôshiba and show that the new features of the effect are compatible with the previous observations.

Miller and Abrahams[5] showed that the transition rate for phonon-induced tunneling of an electron between two donors, differing slightly in energy due to the presence of an ionized acceptor in their vicinity (Mott's[6] model), is proportional to the square of its resonance energy, $|W|^2$. Mikoshiba[4] followed essentially the treatment of Miller and Abrahams in his calculations of the resonance energy but used wave functions derived by including in the Hamiltonian a term quadratic in the magnetic field $\mathbf{H}$. His wave functions decreased in spatial extent as the magnetic field increased (size effect). The magnetic field also introduces a phase difference between the wave functions of neighboring donors (phase effect). Because of mathematical difficulties Mikoshiba treated the size and phase effects separately and considered only the component of the donor wave function derived from one conduction-band valley. The resonance energies for the size effect $W^{(s)}$ and the phase effect $W^{(f)}$ were then squared and averaged over pairs of donors to yield quantities proportional to the transition rate for electron jumping, i.e.,

$$\langle|W_p{}^{(s)}|^2\rangle_{\rm av}\cong\langle|W_{p0}|^2\rangle_{\rm av}\exp\left\{-\frac{1}{48}\frac{\kappa R^3}{m_t{}^*c^2}H^2\cos^2\varphi_p\right\}f_1, \tag{1}$$

$$f_1=\frac{9}{16}\left\{\int_0^1 dx(1+x^2)\exp\left[-\frac{1}{32}\frac{\kappa R^3x^2}{m_t{}^*c^2}H^2\cos^2\varphi_p\right]\right\}^2,$$

* Work supported by the Advanced Research Projects Agency.
† On leave of absence from Institute of Physics, Polish Academy of Sciences, Warsaw, Poland.
[1] R. J. Sladek and R. W. Keyes, Phys. Rev. 122, 437 (1961).
[2] C. Yamanouchi, J. Phys. Soc. Japan 18, 1775 (1963).
[3] W. W. Lee and R. J. Sladek, Bull. Am. Phys. Soc. 10, 546 (1965); W. W. Lee, thesis, Purdue University, 1966 (unpublished).
[4] N. Mikoshiba, Phys. Rev. 127, 1962 (1962).
[5] A. Miller and E. Abrahams, Phys. Rev. 120, 745 (1960).
[6] N. F. Mott and W. D. Twose, Advan. Phys. 10, 107 (1961).